DEPARTMENT OF THE INTERIOR
UNITED STATES GEOLOGICAL SURVEY

GEOCHEMICAL EVALUATION OF FELSIC PLUTONIC ROCKS IN THE EASTERN AND SOUTHEASTERN ARABIAN SHIELD KINGDOM OF SAUDI ARABIA

by

Edward A. du Bray, James E. Elliott,
and Douglas B. Stoeser

U.S. Geological Survey
Open-File Report 83-369

Prepared for:

Ministry of Petroleum and Mineral Resources
Deputy Ministry of Mineral Resources
Jiddah, Kingdom of Saudi Arabia
1403 AH 1983 AD

1983

CONTENTS

ILLUSTRATIONS
[Plates are in pocket]

TABLES

GEOCHEMICAL EVALUATION OF FELSIC PLUTONIC ROCKS IN THE EASTERN AND SOUTHEASTERN ARABIAN SHIELD, KINGDOM OF SAUDI ARABIA

by

Edward A. du Bray, James E. Elliott,1/

and Douglas B. Stoeser

ABSTRACT

In a geochemical evaluation of the eastern and southeastern Arabian Shield, which included collection of 696 rock samples and 694 pan concentrate samples, a province of tin-anomalous granitoid plutons was defined. Pan concentrates collected in and around these plutons were enriched in tin and tungsten relative to the concentrate population. Rock samples of these leucocratic, muscovite-bearing, peraluminous granites contained anomalously high concentrations of lithium, fluorine, beryllium, lead, rubidium, niobium, yttrium, tin, bismuth, silver, and tungsten.

Ten tin-anomalous plutons were located in the study area. The plutons are typically small, less than 10 km^2 in areal extent, and circular to elliptical in plan view. The resource potential of these latest Proterozoic plutons has not been established; economically exploitable concentrations of tin, tungsten, molybdenum, or zinc may be present, and followup studies are warranted. Further, two of the plutons are characterized by higher than normal total-count radioactivity and have potential for uranium, thorium, or rare-earth element deposits.

INTRODUCTION

Previous work and background

Geochemical surveys conducted during early exploration of the eastern and southeastern Arabian Shield demonstrated that the region contains areas having potential for mineral deposits. An unpublished geochemical reconnaissance of the area by P. K. Theobald of the U.S. Geological Survey, Jiddah, included analysis of 2,571 pan concentrate samples and 5,260 -30 to + 80 mesh wadi-sediment samples and identified several areas containing anomalous amounts of tin, tungsten, and (or) molybdenum. Whitlow (1968a,b,c,d) added definition to these anomalies in a series of geological-geochemical 1:100,000-

1/ U.S. Geological Survey, Denver, Colorado

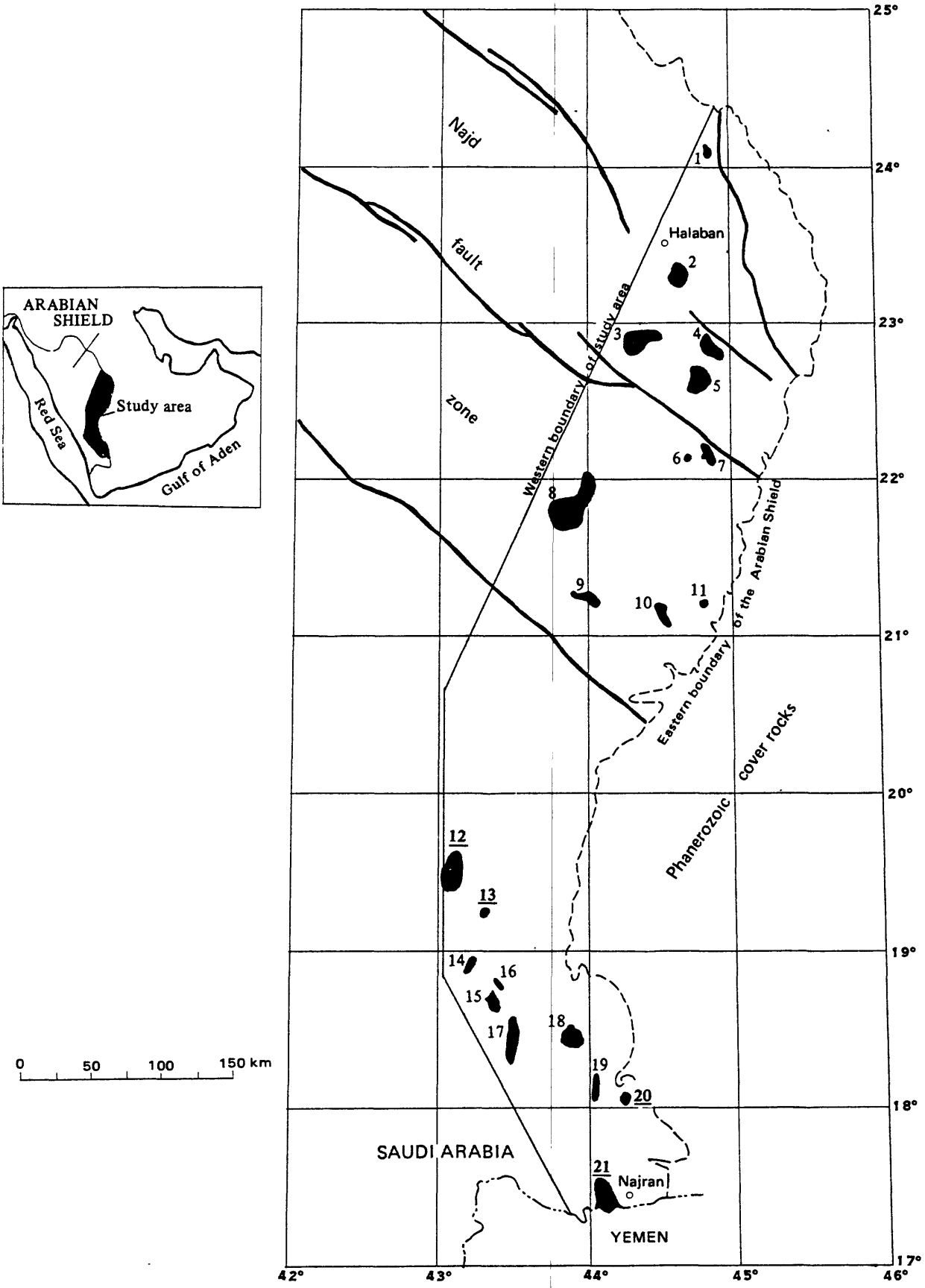

Figure 1.–Index map showing the location of the felsic plutonic rocks study area in the eastern and southeastern Arabian Shield. Numbered localities refer to plutons described in table 2. Underlined locality numbers indicate alkali granites, all other localities are muscovite granites. Heavy unlabeled lines indicate major faults.

scale quadrangle maps. Theobald (1970) suggested that the monzogranite and granodiorite that occur in the Al Kushaymiyah region, east-central Arabian Shield (fig. 1), have potential for a porphyry-molybdenum deposit. Following Theobald's recommendations, Dodge (1973), Theobald and Allcott (1973), and Dodge and Helaby (1975) completed detailed assessment studies at Al Kushaymiyah.

In 1977 J. E. Elliott, U.S. Geological Survey Saudi Arabian Mission, initiated a more detailed reconnaissance geochemical exploration program in the eastern and southeastern Arabian Shield, which concentrated on felsic plutonic rocks. The elements (and the principal economic minerals) sought were tin (cassiterite), tungsten (wolframite and scheelite), and molybdenum (molybdenite and powellite). Elliott (unpublished data, 1982) identified several tin-bearing granitoid plutons during preliminary work in the eastern and southeastern Arabian Shield. The monzogranite (plutonic nomenclature in this report is that of Streckeisen, 1976) exposed at Jabal al Gaharra is one of these and was studied in detail (Elliott, 1980). Elliott indicated that this two-mica leucomonzogranite, although tin-bearing, does not contain economic tin deposits at the present level of exposure.

Chappell and White (1974), Tischendorf (1977), and Groves and McCarthy (1978) considered the particular geochemical and petrologic characteristics of granitoid plutons that may host tin and (or) tungsten deposits. These S-type granites, as defined by Chappell and White (1974), have the following characteristics:

1. biotite and (or) muscovite are the only volumetrically significant nonquartz or nonfeldspar phases

2. initial $^{87}Sr/^{86}Sr$ ratios greater than 0.708, suggesting genesis by remelting of preexisting continental crust

3. molar $Al_2O_3/(Na_2O+K_2O+CaO)$ greater than 1.1, that is, strongly peraluminous, which is reflected by CIPW normative corundum greater than 1 percent

4. composition restricted to magmas with SiO_2 greater than 72 weight percent

5. trends on variation diagrams irregular

6. Na_2O normally less than 3.2 percent in rocks with approximately 5 percent K_2O

Although Chappell and White (1974) created the I-type and S-type distinction for a small group of Australian granitoid rocks, the characteristics that they attribute to the latter

type define an important class of granitoids, and geoscientists throughout the world have adopted their classification. In global usage and in this study the peraluminous plutons that have been labeled S-type may not meet all of the original criteria of Chappell and White but they usually meet a majority. Chappell and White proposed genesis of S-type granites by melting sedimentary rocks and genesis of I-type by melting igneous rocks. However, the genetic implication inherent in the use of I- and S-type nomenclature is at present seldom considered by most geoscientists, and the use of this nomenclature in this report does not propose genesis of these rocks by melting sedimentary rocks but only indicates the existence of chemical and petrographic similarities between the plutons so identified here and S-type granites as defined by Chappell and White (1974).

Groves and McCarthy (1978) presented the physicochemical conditions that favor the genesis of metal-enriched magmas. The results of Elliott (in press; unpublished data, 1982) suggest that the eastern and southeastern Arabian Shield may contain similar mineralized S-type granites.

In addition to the S-type granites described above, peralkaline granites of possible economic significance are widespread in the Arabian Shield (Stoeser and Elliott, 1980). In particular, Drysdall (1979) and Douch and Drysdall (1980) have identified highly radioactive microgranitic apophyses, associated with larger peralkaline plutons, in the northwestern Hijaz region of the Arabian Shield. These apophyses are enriched in niobium, tantalum, tin, thorium, yttrium, zirconium, and zinc. Drysdall (1979) suggested that these apophyses may be similar to the younger granites of Nigeria and as such are possible hosts to tin-zinc deposits. He also indicated that they bear some resemblance to metasomatized granites in eastern Egypt that contain niobium, tantalum, tin, and tungsten deposits. Because peralkaline granites also are found within the study area, there is potential for this type of deposit as well.

This study was performed by the U.S. Geological Survey as part of a work agreement with the Saudi Arabian Ministry of Petroleum and Mineral Resources, in order to complete a program of reconnaissance wadi-sediment and rock sampling of the felsic plutons in the eastern and southeastern Arabian Shield. The geochemical and petrographic characteristics of these rocks were established, and geochemically anomalous plutons were noted. A special effort was made to identify and characterize all peraluminous and peralkaline plutons and to define target areas that merit further exploration.

Setting

Much of the area has been reduced to a peneplain, and large mountain masses are uncommon. Isolated and coalescing inselbergs rise above the plain to break the otherwise monotonous surface. A relatively well integrated drainage system, a remnant of wetter times, covers most of the area, but wadis remain dry except during very rainy periods. Peneplained surfaces are covered in most places by at least several meters of sand and gravel, and parts of the area are covered by sand seas several hundreds of meters thick.

ACKNOWLEDGMENTS

The authors thank the chief of the U. S. Geological Survey Saudi Arabian Mission computer section, G. I. Selner, for writing statistical programs, processing data, and interfacing an X-ray fluorescence spectrometer with its online reduction minicomputer. Directorate General of Mineral Resources (DGMR)-USGS chemists, K. J. Curry, Ali Bone, Ahmed Baraja, Najeeb Nabhan, Jamal Sombol, and Hassan Mousa performed semiquantitative and quantitative analytical work. Ali Jarbarti and Ali Dualeh panned all wadi-sediment samples, and Ali Jabarti and Ahmed Hamdan Al Bazli performed point counts on all stained slabs. Finally, the authors would like to thank W. J. Moore and J. S. Stuckless, USGS, for their thoughtful reviews.

REGIONAL GEOLOGY

The eastern and southeastern Arabian Shield is underlain by Precambrian intrusive and metamorphic rocks. The intrusive rocks range in composition from diorite and gabbro to alkali-feldspar granite, but granodiorite and monzogranite are most extensive. The study area is underlain by several hundred granitoid plutons that form an interlocking mosaic, locally separated by roof pendants. A group of latest Proterozoic, postorogenic granitoid plutons comprises about 25 percent of the area underlain by plutonic rocks (Greenwood and Brown, 1973). This group of postorogenic plutons ultimately proved to have the highest favorability for mineral deposits.

The principal metamorphic rocks in the study area are those of the Abt formation in the northern part of the area and of the Murdama and Halaban groups throughout. These rocks were thermally metamorphosed at greenschist- and lower amphibolite-facies conditions during pluton emplacement. Complex structural history is preserved in these layered rocks, which were deformed during the compressional events that accompanied cratonization of the Arabian Shield, and each metamorphic group contains characteristic structural styles and patterns attributable to multiple deformation.

The Najd fault zone is one of the most significant structural features in the study area. Many faults, along which there has been small to moderate offset, and two major northwest-trending Najd faults cut the northern part of the area.

Diabase, basalt, andesite, and rhyolite dikes transect rocks of the Arabian Shield, and many swarms, each with a characteristic trend, are represented. Aplite and pegmatite dikes commonly cut the intrusive rocks.

The preceding is a superficial treatment of the regional geology. U.S. Geological Survey map I-270 A (U.S. Geological Survey and Arabian American Oil Company, 1963) provides an overview of Arabian Shield geology, and greater geologic detail is available in the 1:100,000-scale quadrangle maps covering the area. U.S. Geological Survey Mission Interagency Report 400 (U.S. Geological Survey, 1980/1982) provides an index to quadrangle mapping completed as of Muharram 1, 1401 (November 9, 1980). Detailed regional geologic and synthesis studies of the Arabian Shield include those by Schmidt and others (1979), Fleck and others (1980), and Greenwood and others (1980, 1982).

METHODS AND DATA PRESENTATION

A very large region was examined during this study, and using the data gathered, an attempt was made to identify plutons that showed an affinity for the mineral-deposit types considered by Chappell and White (1974), Tischendorf (1977), and Groves and McCarthy (1978). Each pluton identified on the 1:100,000-scale geologic maps of the area (U.S. Geological Survey, 1980/1982) was sampled at one location and generally at several. Plutons previously identified as anomalous by Elliott (unpublished data, 1982) were more thoroughly sampled. Sediment and rock samples were collected for chemical analysis and for petrographic studies. Total-count radiation readings were recorded at each sample location.

Geochemical sampling

All sampling subsequent to Elliott's preliminary work was completed in 6 weeks of helicopter-assisted fieldwork between February 1980 and January 1981. At each sample location approximately 10 kg of medium- to coarse-grained wadi sediment and about 1 kg of representative rock from nearby outcrop were collected for chemical analysis. Another rock sample was collected at each location for thin sectioning and preparation of a stained slab.

Sample locations were predetermined on the basis of local geology. Using 1:100,000-scale geologic maps and photomosaics, locations were identified that insured homogeneous source terrane and easy availability of both wadi sediment

and rock. A total of 696 locations were sampled for this study: 123 by Elliott in 1978 and 1979 and 573 subsequently by du Bray. All sample locations are shown on plates 1-3. Detailed sample location maps and geochemical data are available in base data file USGS-DF-01-05, on file in offices of the U.S. Geological Survey, Jiddah, Saudi Arabia.

Scintillometry

A total-count scintillometer having a cylindrical (38.1 mm x 38.1 mm) sodium iodide detection crystal was used to measure radioactivity at each sampling site. At each site, the instrument was set on a planar outcrop and allowed to equilibrate before the reading was taken. Results of the radiometric survey are plotted on figure 2.

Sample processing

Each 10-kg wadi-sediment sample was split approximately into a 7.5-kg fraction and a 2.5-kg fraction. The latter was archived for future reference. The heavy minerals were concentrated in the former using a gold pan and standard panning techniques.

A -30 to +80 mesh bulk wadi-sediment sample was produced by splitting and sieving the archived sample fraction of all 123 samples collected by Elliott and the first 188 samples collected by du Bray. This work resulted in a sample media efficiency study (du Bray, 1981), which demonstrated that because of dilution by quartz and feldspar, the -30 to +80 mesh fraction of wadi sediment conveys insufficient information to warrant further analysis of this sample medium. Analysis of this sample medium was discontinued, but preparation and analysis of pan concentrates continued.

Chemical analysis

All pan concentrates were submitted to the DGMR-USGS chemical laboratory, Jiddah, for 30-element semiquantitative spectrographic analysis (table 1). Semiquantitative spectrographic data reported here do not represent absolute analytical values but rather parts per million (ppm) or weight percent to the nearest number in the series 1.0, 0.7, 0.5, 0.3, 0.2, 0.15, 0.1, and so forth, which represents the approximate midpoint of group data intervals on a geometric scale. In addition to 30-element semiquantitative spectrographic analysis, determinations of fluorine using the selective-ion-electrode method, lithium using atomic absorption, and tungsten using colorimetry were made for rock samples.

Additional trace-element analyses were completed for all rock samples using the U.S. Geological Survey X-ray fluorescence multichannel spectrometer; sample excitation was

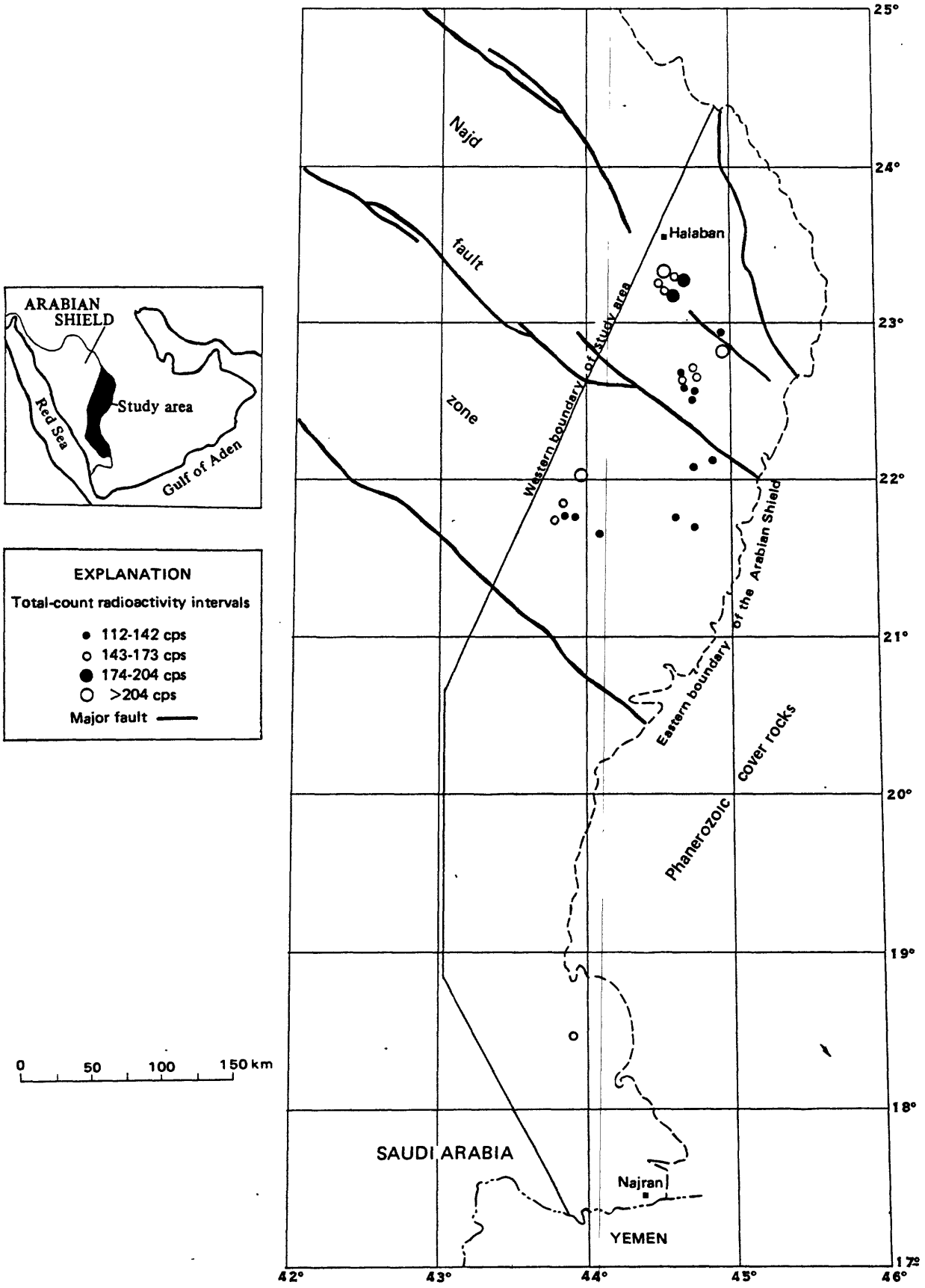

Figure 2.--Map showing the results of total-count radiation measurements made at sample sites occupied by du Bray. Only values in excess of two standard deviations (one standard deviation = 31 counts per second) greater than the mean (50 counts per second) of all measurements are shown. The intervals indicated in the explanation represent values greater than the mean by 2-3 standard deviations, by 3-4 standard deviations, by 4-5 standard deviations, and by 5 or more standard deviations.

Table 1.--*Elemental geometric means of semiquantitative spectrographic data for rock and pan concentrate samples collected in the eastern and southeastern Arabian Shield*

[Results are in ppm, except for Fe, Mg, Ca, and Ti, which are in weight percent. N.D. indicates not determined. Leader indicates element undetected in all samples. Means were calculated using the method of Cohen (Miesch, 1967); when this was not possible, the geometric mean of unqualified data is given (*). Geometric means for Ag, Bi, Mo, Sn, W, and Zn are based on very few unqualified values and have little significance. Samples in northern group were collected between lat 22° N. and 24°30' N., in central group between lat 19°30' N. and 22° N., in southern group between lat 17°45' N. and 19°30' N. Samples collected by Elliott are located throughout study area. Number of samples on which means are based are shown in parentheses. Average granite values from Krauskopf, 1967]

	Rock samples					Average	Pan concentrate samples				
	North (188)	Central (200)	South (183)	Elliott (125)	Total (696)	granite (2,327)	North (190)	Central (200)	South (181)	Elliott (123)	Total (694)
Fe	1.51	1.53	1.73	I.13	1.50	3.09	8.42*	6.67*	8.98*	6.32*	7.60*
Mg	0.26	0.25	0.20	0.05	0.17	0.81	1.10	1.33	1.67	0.69	1.19
Ca	1.42	1.08	1.09	.37	.96	1.89	2.64	3.27	3.28	1.10	2.55
Ti	.12	.13	.13*	.02	.11*	.34	0.71*	0.91*	0.91*	.70*	.79*
Mn	280	364	323	380*	331*	400	1,453*	1,113	1,330	1,544*	1,329
Ag	.6*	—	—	.2	1.0*	.04	—	—	—	—	—
B	7	18*	7	12*	5	15	6	6	11	17	8
Ba	214	311	390	42	223	600	136	223	218	214	192
Be	1	2	1	3	2	5	1	2	1	2	1
Bi	—	—	—	25*	25*	.18	1	—	—	27*	21*
Co	1	1	.5	11	1	1	11	8	10	19	11
Cr	147	155	202	220	175	4	410*	367	488	440	421*
Cu	16	18	14	13	16	10	53	42	26	35	38
La	17	21	27	17	21	40	85*	45	61	66	63*
Mo	—	9*	3	2	1	2	1	6*	2	2	1
Nb	3	23*	27*	18	5	20	43*	27*	12	89*	42*
Ni	3	3	3	4	3	.5	21	27	35	40	29
Pb	13	12	12	23	14	20	16	7	13*	7	8
Sc	3	2	1	1	2	5	11	15	21	18	16
Sn	31*	20*	46*	8	.2	3	34*	20*	18*	98*	34*
Sr	113	111	136	33	103	285	90	171	180	162	149
V	22	19	19	18	20	20	205	199	173	156	185
W	—	—	—	—	—	2	90*	—	—	90*	90*
Y	16	13	14	46	17	40	95	40	62	64	62
Zn	—	—	245*	291*	282	40	—	—	—	—	—
Zr	83	96	122*	93	100	180	780*	911*	832*	510*	775*
Ft	767	470	614	1,853	836	850	N.D.	N.D.	N.D.	N.D.	N.D.
Lit	34	18	18	157	47	30	N.D.	N.D	N.D.	N.D.	N.D.
Wt	18	10	—	133	24	2	N.D.	N.D.	N.D.	N.D.	N.D.

† Determined by wet chemistry; arithmetic mean calculated.

achieved using a Cd-109 radioisotope source. Accurate, high-precision determinations were made for rubidium, strontium, zirconium, niobium, and yttrium (Elsass and du Bray, unpub. data). The X-ray fluorescence data represent discrete values within the limits of analytical precision. The analytical precision of the analyses is ±5 percent of the amount indicated. Spectrographic, quantitative, and X-ray fluorescence data for pan concentrates and rocks are summarized in frequency histograms (figs. 3-5). A complete listing of the data used for this report is available in USGS base data file USGS-DF-01-05. The sample-numbering scheme used in this study is explained in this data file. Inquiries regarding this data file should be made to the U.S. Geological Survey, Jiddah, Saudi Arabia.

Table 1 shows the geochemical variation on a regional basis within the study area and compares the chemistry of granitoids of the study area with that of an average granite (Krauskopf, 1967). The statistical treatment that follows would be futile if the entire study area or a major part of it was geochemically anomalous. Comparison of the "Total" column for rock samples with the "Average granite" column (table 1) indicates that this is not the case. With the exception of iron, magnesium, calcium, chromium, barium, and strontium, the granitoids exposed in the study area are chemically very similar to the average granite. Considering that the analyses presented here are semiquantitative, the agreement is good.

Iron, magnesium, calcium, titanium, bismuth, yttrium, fluorine, and lithium contents of rock samples collected by Elliott vary significantly from the regional means, but this can be attributed to the large number of samples (43) collected from the Jabal al Gaharra tin-bearing monzogranite (Elliott, in press). Discounting these samples, there is not much geochemical variation of rock samples from various parts of the study area. Elliott's pan concentrates seem similarly affected by the dense sampling at Jabal al Gaharra. Discounting those, the composition of the pan concentrates also appears to be relatively homogeneous throughout the eastern Arabian Shield. In no case is there a regional variation of much more than one spectrographic reporting interval. A significantly more rigorous statistical evaluation of regional geochemical variation could be attempted, but considering the nature of the data and the effort that would be required, this would be beyond the scope of the study.

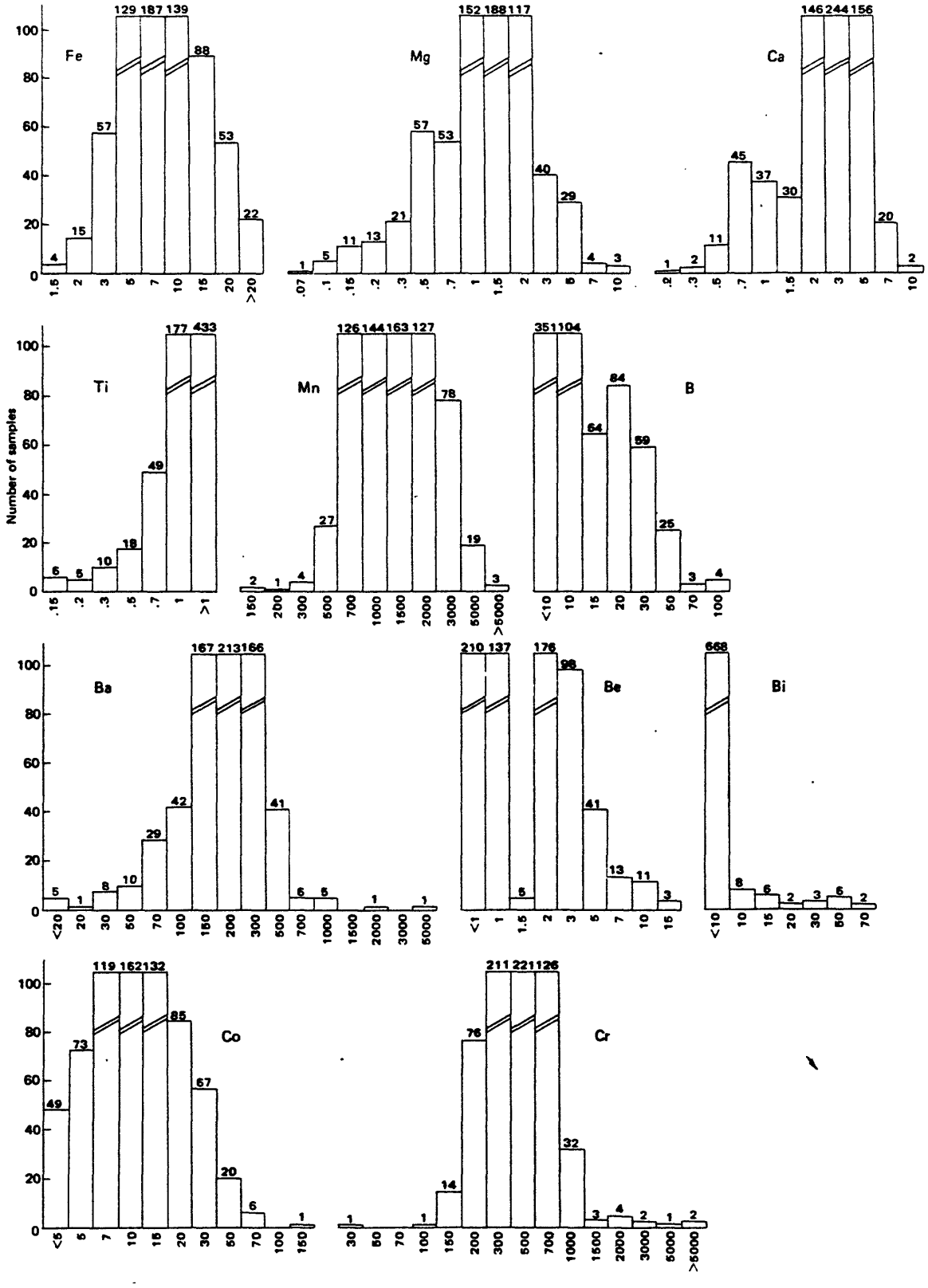

Figure 3.–Frequency distribution of semiquantitative spectrographic analyses for 694 pan concentrate samples collected in the eastern and southeastern Arabian Shield. Iron, magnesium, calcium, and titanium concentrations in percent, all others in parts per million. Limits of concentration intervals are in the series .083, .12, .18, .26, .38, .56, .83, 1.2, and so forth; data are plotted against concentration-interval midpoints 0.1, .15, .2, .3, .5, .7, 1.0, and so forth, respectively. Number of samples in each interval is indicated.

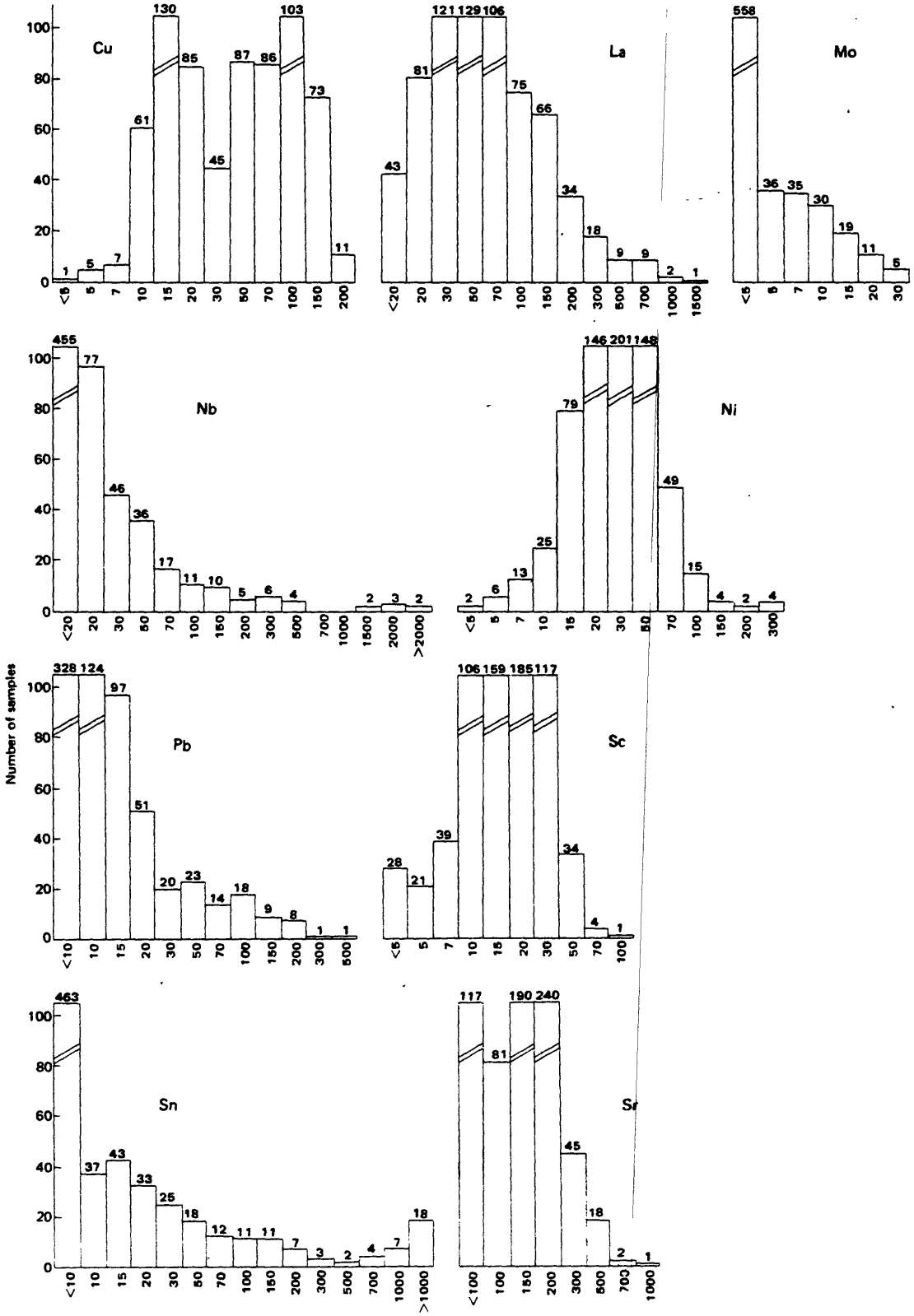

Figure 3.– Continued

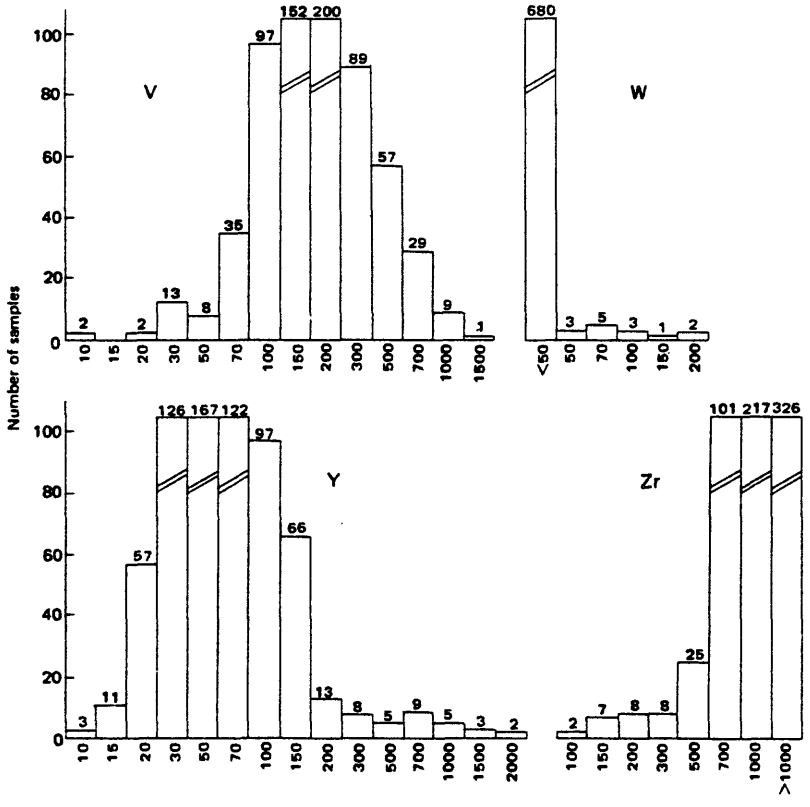

Figure 3.– Continued

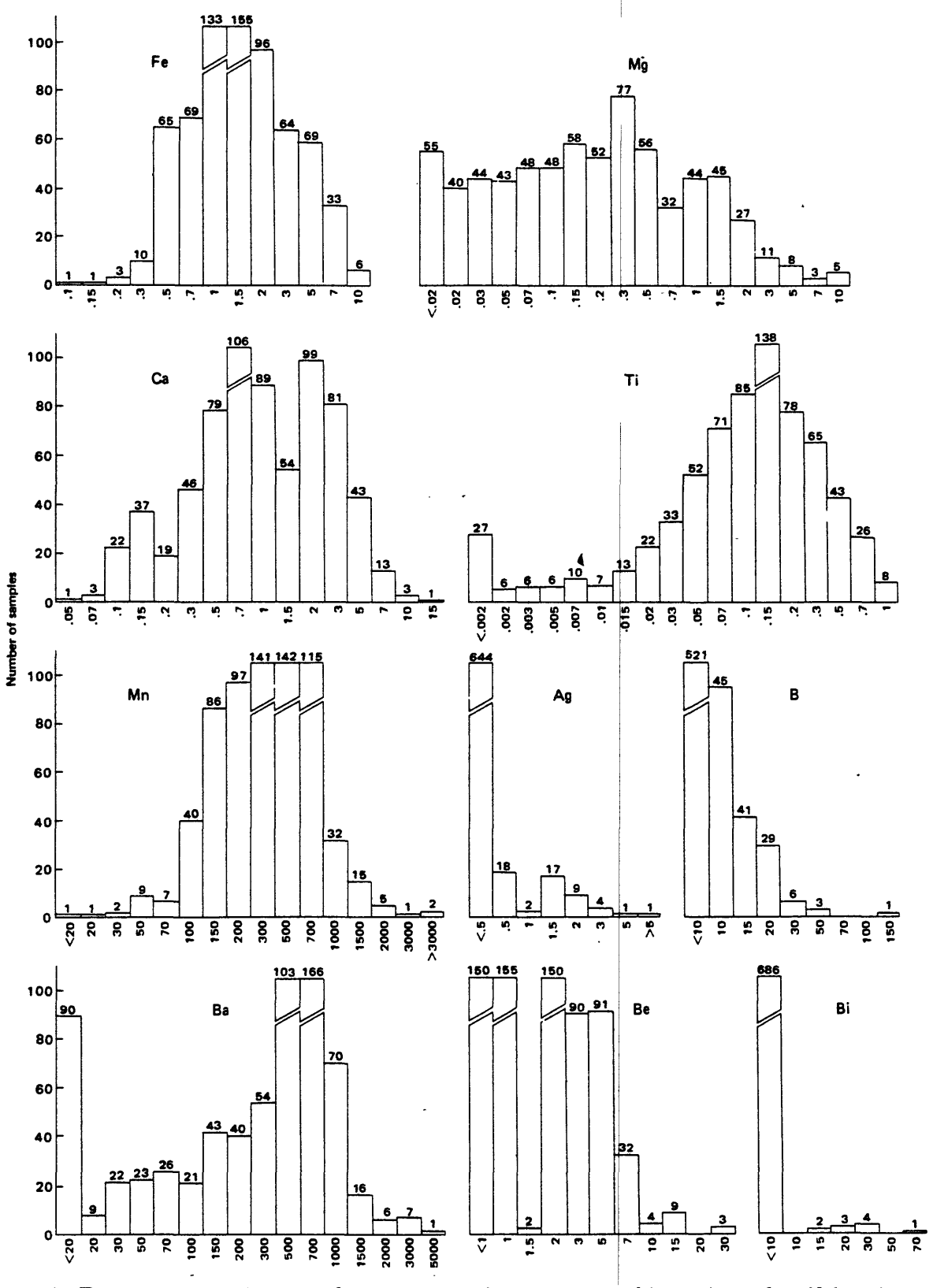

Figure 4.–Frequency distribution of semiquantitative spectrographic analyses for 696 rock samples collected in the eastern and southeastern Arabian Shield. Iron, magnesium, calcium, and titanium concentrations in percent, all others in parts per million. Limits of concentration intervals are in the series .083, .12, .18, .26, .38, .56, .83, 1.2, and so forth; data are plotted against concentration interval midpoints 0.1, .15, .2, .3, .5, .7, 1.0, and so forth, respectively.

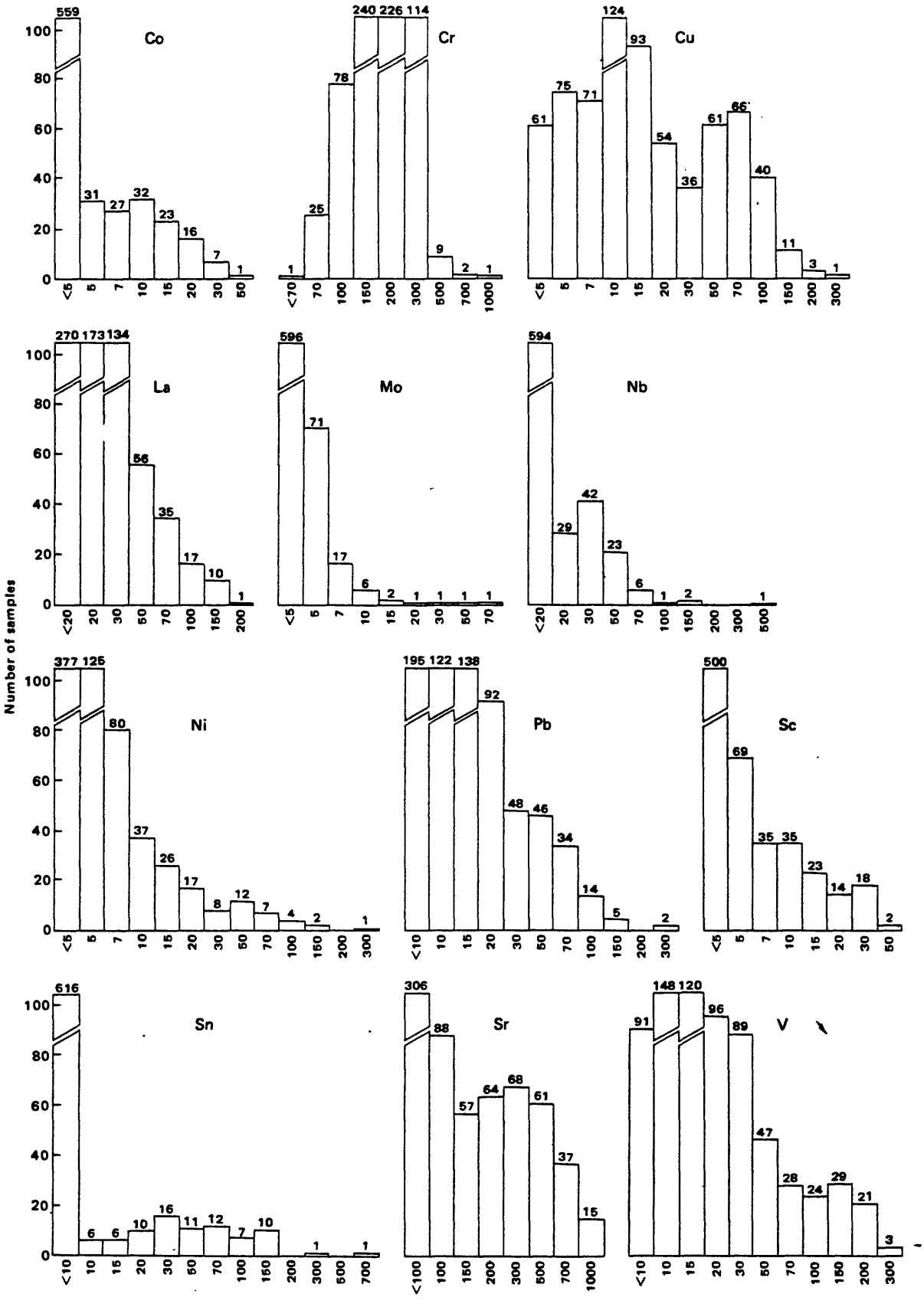

Figure 4.– Continued

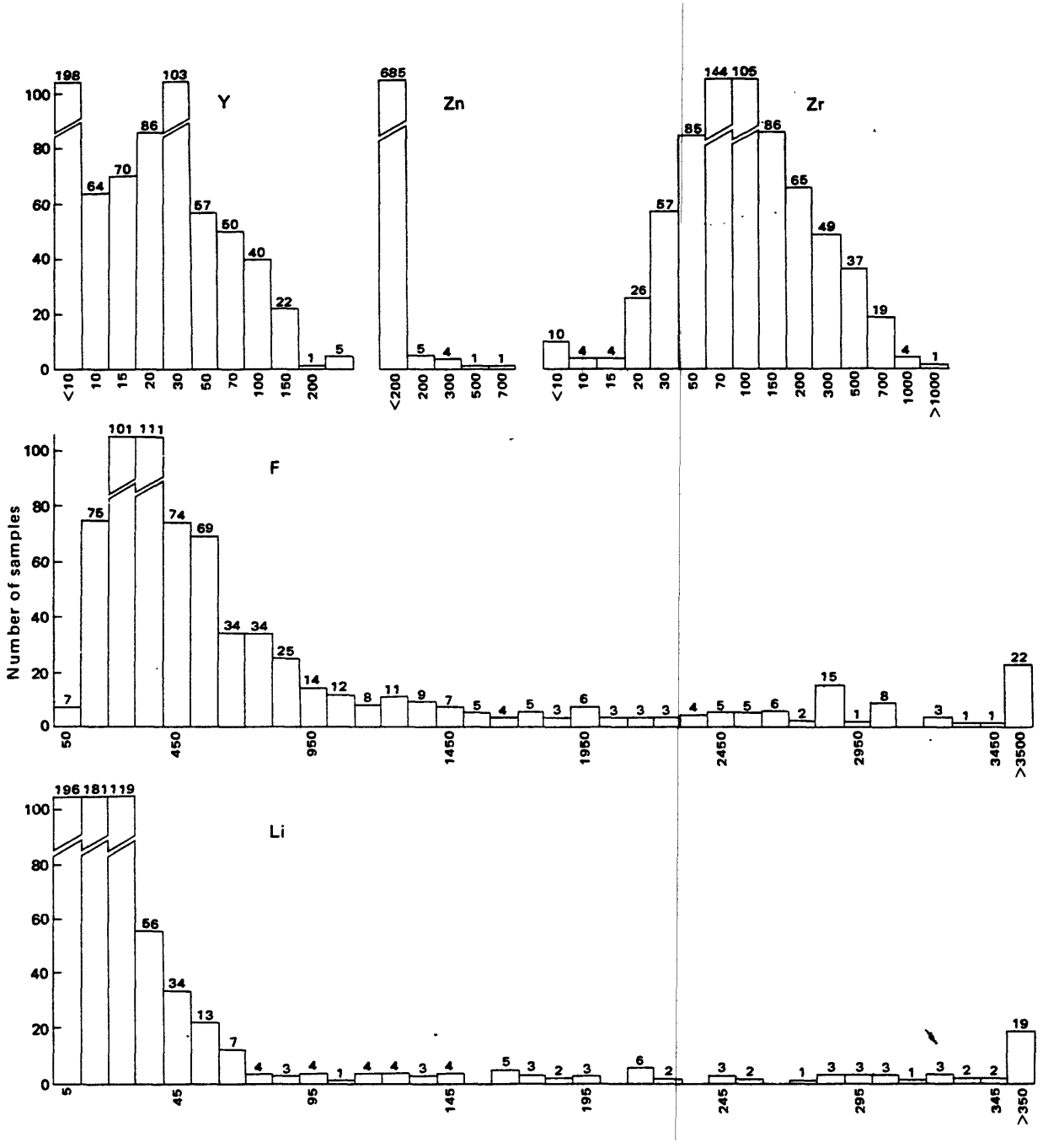

Figure 4.– Continued

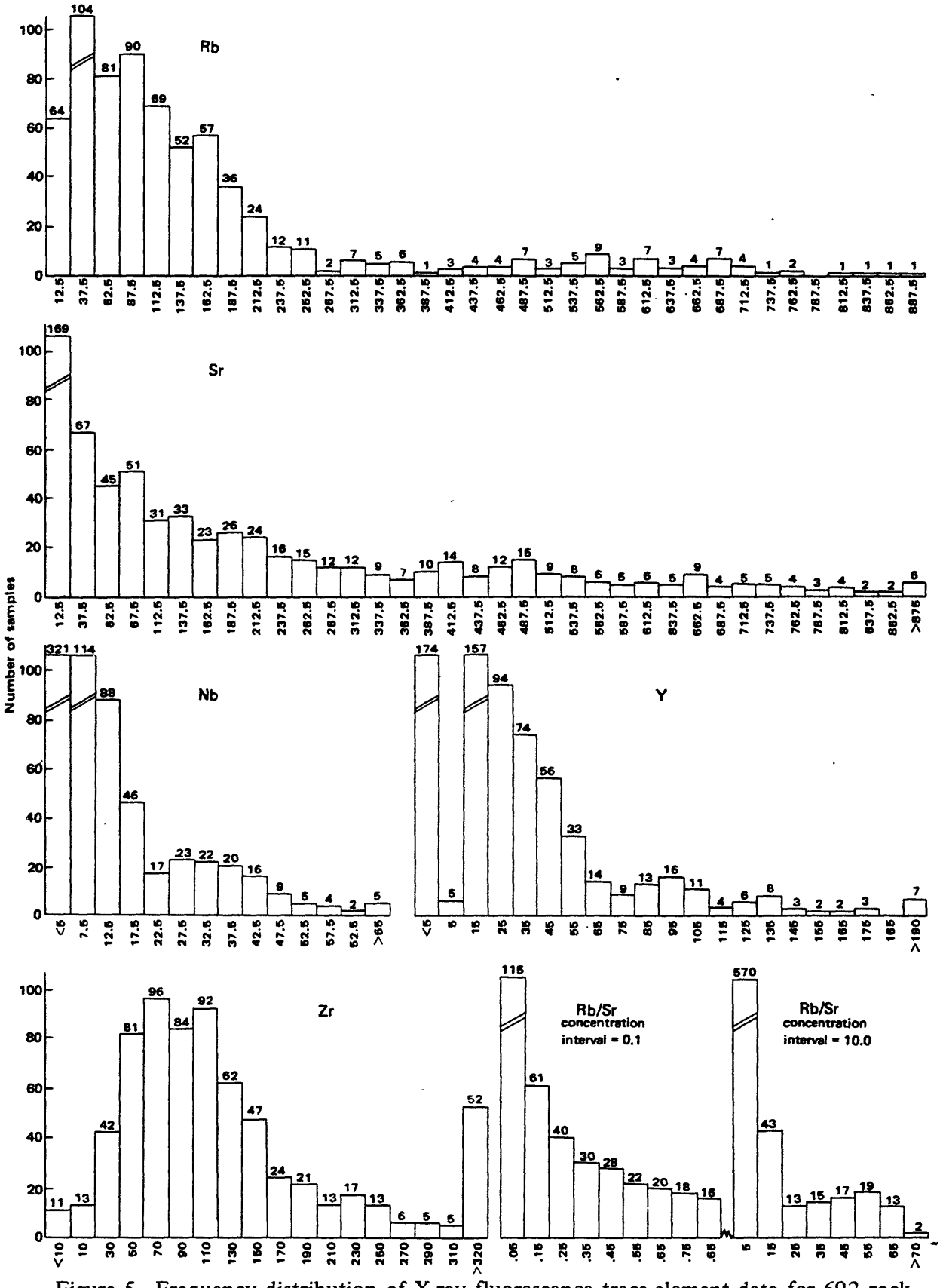

Figure 5.–Frequency distribution of X-ray fluorescence trace-element data for 692 rock samples collected in the eastern and southeastern Arabian Shield. Concentration intervals have the following widths: rubidium, 25 ppm; strontium, 25 ppm; yttrium, 10 ppm; zirconium, 20 ppm; niobium, 5 ppm; Rb/Sr 0.1 and 10. Data are plotted against interval midpoints Number of samples in each interval is indicated.

Petrography

Petrographic study of rock samples included modal analysis of stained slabs and examination of thin sections. Between 350 and 700 points were counted on each stained slab, averaging about 60 cm^2 of surface area; each point was assigned to one of the categories: quartz, alkali feldspar, plagioclase, mafic minerals. Results of the modal analyses are plotted on QAP (Streckeisen, 1976) and QFM ternary diagrams (figs. 6, 7). The mafic and accessory mineral suites and microscopic textural features of rock samples were determined by examination of thin sections.

The felsic plutonic rocks of the eastern and southeastern Arabian Shield can be divided on the basis of petrography into five classes (in order of abundance): 1) equigranular biotite monzogranite, 2) equigranular biotite and (or) hornblende granodiorite, 3) monzogranite and granodiorite, both of which contain biotite and megacrystal microcline; 4) alaskitic muscovite granite, and 5) alkali granite. Of these classes, only the alaskitic muscovite granites (13 plutons) and alkali granites (4 plutons) appear favorable for mineral deposits. The locations of these plutons are shown in figure 1, and their petrography is tabulated in table 2.

The alaskitic muscovite monzogranites are leucocratic and medium grained and typically have hypidiomorphic-equigranular to xenomorphic-granular textures. Porphyritic varieties are rare. The potassium feldspar is nonperthitic microcline, amazonitic in some plutons, and the plagioclase is unzoned, polysynthetically twinned albite. Biotite and muscovite are present in varying proportions, although muscovite is dominant in the smaller plutons. Spessartine garnet (as much as 1 modal percent) is present in seven of the plutons (table 2). Ilmenite is the characteristic oxide mineral but averages less than 0.1 percent. Other characteristic accessory minerals are zircon, apatite, and fluorite. The muscovite granites are chemically peraluminous, that is, molar $Al_2O_3/(CaO+Na_2O+K_2O)$ is greater than 1 (du Bray, 1982). They also have the petrographic and trace-element chemical characteristics of S-type granites.

The alkali granites usually contain aegerine-augite and either arfvedsonite or arfvedsonite-riebeckite. In the southeastern Arabian Shield these granites are hypersolvus, medium- to coarse-grained perthite alkali-feldspar granites and syenogranites in which the felsic minerals crystallized early and the mafic silicate minerals tend to be late interstitial. Chief accessory minerals are magnetite, fluorite, allanite, and abundant zircon. The alkali granites are chemically peralkaline, that is, molar $(Na_2O+K_2O)/Al_2O_3$ is greater than 1. Further information regarding the peralkaline granites of the Arabian Shield is presented by Stoeser

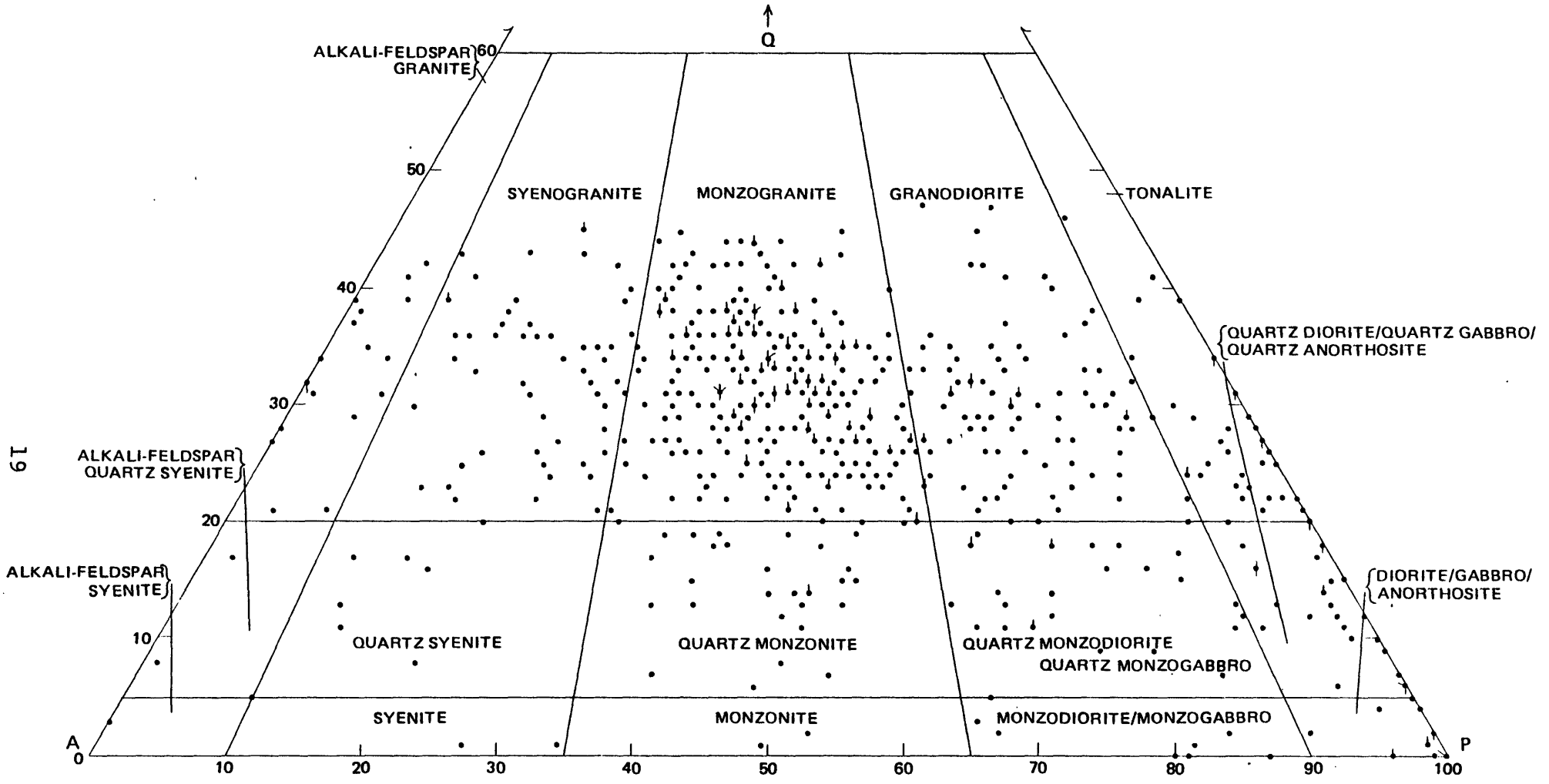

Figure 6.–Quartz-alkali feldspar-plagioclase feldspar (QAP) ternary diagram showing the modal composition of 696 granitoid rock samples collected in the eastern and southeastern Arabian Shield. Each dot represents one sample. Each bar on a dot represents an additional sample with the same modal composition. Lithologic nomenclature is that of Streckeisen (1976).

Table 2.--*Petrography of granitoid plutons of economic interest in the eastern and southeastern Arabian Shield*

[Locality numbers keyed to fig. 1]

Locality number	Pluton name	Petrographic characteristics
1	Jabal al Ehn monzogranite	Hypidiomorphic, inequigranular to subporphyritic, medium-grained monzogranite containing biotite and muscovite
2	Jabal Sabhah monzogranite	Hypidiomorphic, inequigranular, medium-grained monzogranite containing biotite and muscovite
3	Granites of the Uyaijah ring structure in the Kushaymiya complex	Hypidiomorphic, porphyritic, medium-grained microcline granodiorite host, surrounded by a ring dike of hypidiomorphic-xenomorphic to granular, medium-grained seriate leucogranite and intruded by a core stock of hypidiomorphic-granular, seriate, medium-grained granite and granodiorite
4	Hassat ibyn Huwail granite	Hypidiomorphic, inequigranular to subporphyritic, medium-grained granite containing biotite and muscovite
5	Jabal al Hawshah monzogranite	Hypidiomorphic, inequigranular to subporphyritic, medium-grained monzogranite containing biotite and muscovite
6	Jabal as Sitarah monzogranite	Hypidiomorphic to xenomorphic, inequigranular to subporphyritic, medium-grained monzogranite containing biotite and muscovite
7	Jabal Sahah granite	Hypidiomorphic, equigranular, medium- to coarse-grained granite containing biotite and muscovite
8	Granite near Bir Masala	Hypidiomorphic, equigranular, medium-grained granite containing biotite and muscovite
9	Monzogranite near Jabal Tarban	Hypidiomorphic to xenomorphic, inequigranular, medium-grained monzogranite containing biotite, muscovite, garnet, and locally amazonite
10	Monzogranite and granodiorite near Jabal Kebad	Hypidiomorphic, inequigranular, medium-grained monzogranite and granodiorite both containing biotite, muscovite, and garnet
11	Granodiorite near Jabal Mahail	Hypidiomorphic, equigranular, medium-grained granodiorite containing muscovite and garnet

Table 2.--*Petrography of granitoid plutons of economic interest in the eastern and southeastern Arabian Shield*-Continued

Locality number	Pluton name	Petrographic characteristics
12	Granite and alkali granite of the Jabal al Hassir ring complex	Core of hypidiomorphic, inequigranular to subporphyritic, medium-grained biotite monzogranite surrounded by a ring of hypidiomorphic, inequigranular, coarse-grained alkali granite containing perthite, biotite, and arfvedsonite
13	Alkali granite south of Kitmah	Hypidiomorphic, subporphyritic, medium-grained alkali granite containing riebeckite
14	Monzogranite near Wadi Tafshah	Hypidiomorphic, inequigranular, medium-grained gneissic monzogranite containing garnet and muscovite
15	Granodiorite near Madha	Hypidiomorphic, inequigranular, medium-grained gneissic granodiorite containing muscovite, biotite, and garnet
16	Monzogranite and granodiorite near Jabal Zayd	Hypidiomorphic, equigranular, medium-grained monzogranite and granodiorite containing biotite, muscovite, and garnet
17	Wadi al Habbah granodiorite	Hypidiomorphic, inequigranular, medium-grained pegmatitic granodiorite containing biotite, muscovite, and garnet
18	Jabal Bani Bwana granite	Hypidiomorphic, inequigranular to subporphyritic, medium-grained quartz porphyritic granite containing biotite, muscovite, and locally amazonite
19	Jabal al Gaharra monzogranite	Hypidiomorphic, equigranular, medium-grained monzogranite containing biotite and muscovite
20	Granite and alkali granite of the Jabal Ashirah ring complex	Core of hypidiomorphic to xenomorphic, inequigranular, medium-grained biotite monzogranite surrounded by a ring of hypidiomorphic, inequigranular, coarse-grained alkali granite containing perthite, arfvedsonite, biotite, and riebeckite
21	Najran alkali granite	Hypidiomorphic, inequigranular, coarse-grained alkali granite containing perthite, arfvedsonite, biotite, and riebeckite

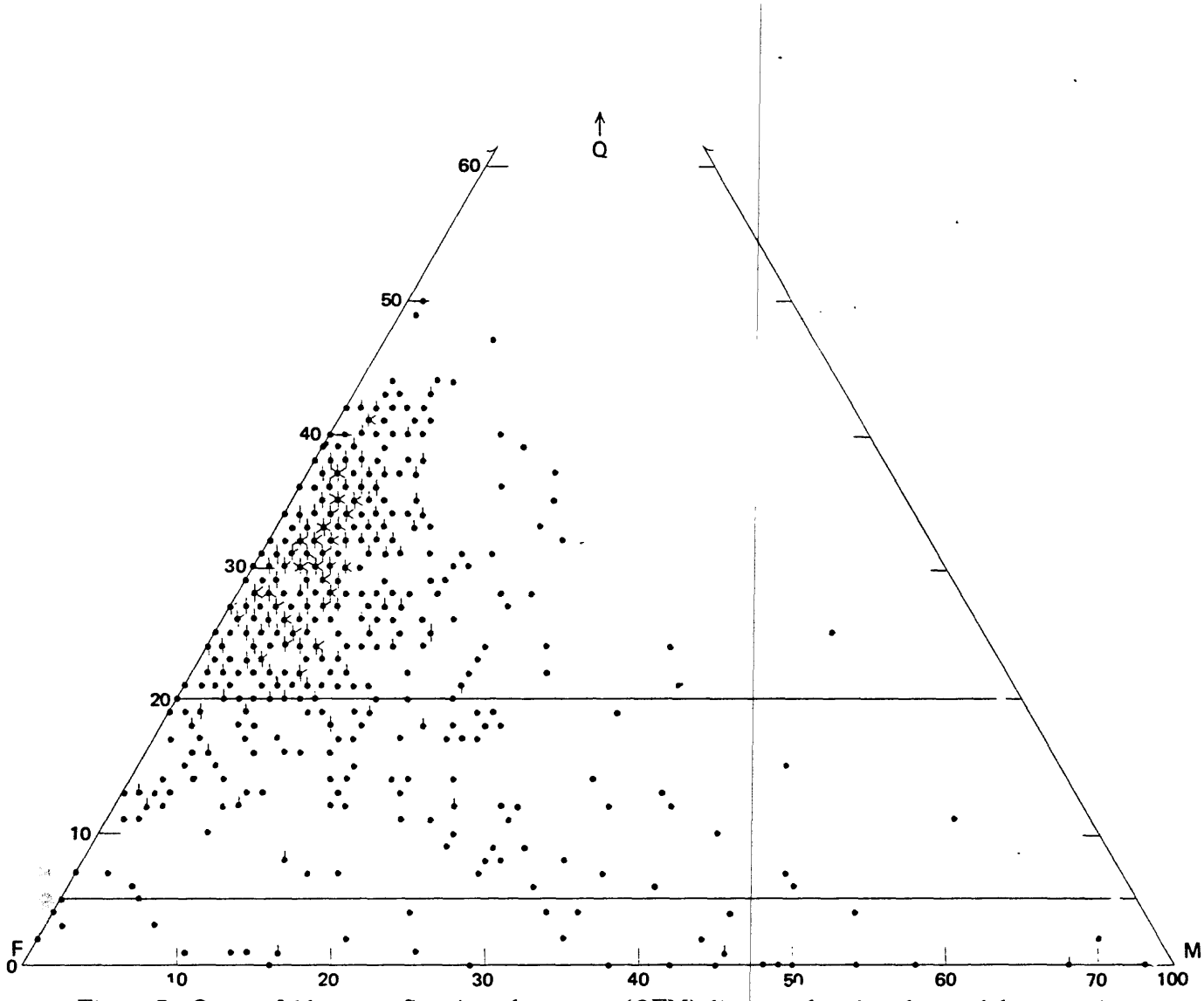

Figure 7.–Quartz-feldspar-mafic minerals ternary (QFM) diagram showing the modal composition of 696 granitoid rock samples collected in the eastern and southeastern Arabian Shield. Each dot represents one sample. Each bar on a dot represents an additional sample with the same composition.

and Elliott (1980). Other studies have shown that the peralkaline granites in the northwestern part of the Arabian Shield have potential for economic deposits of uranium, thorium, tantalum, niobium, and the rare-earth elements (Douch and Drysdall, 1980; Drysdall, 1979). The alkali granites in the study area probably have similar potential.

The alaskitic muscovite granites were found throughout the study area, whereas the alkali granites were found only in the southern half. Both types of granites tend to crop out as round to elliptical plutons in plan view, whereas the majority of the other plutonic rocks tend to occur in very elongated or very irregularly shaped plutons. A detailed study of the petrology of the peraluminous granites is being prepared by du Bray, and the present report concentrates only on the geochemical exploration related to them.

Data evaluation

Definition of anomalous values

The goals in regional geochemical prospecting are to establish background concentration levels and to identify geologic features that are geochemically anomalous. First, however, an anomaly threshold concentration must be established for each element of the geochemical survey. Element threshold concentrations have previously been defined as the arithmetic mean ($\bar{x}$) of the population plus two standard deviations (2σ) (Overstreet, 1978) or as the upper 2.5 percent of all observations (Hawkes and Webb, 1962), but threshold concentrations are more commonly established by visual examination of frequency distribution histograms. None of these methods is very rigorous or very effective with regard to proper threshold concentration identification.

Ahrens (1957) noted that most trace elements found in geologic materials are lognormally distributed. Lognormally distributed populations plot as straight lines if log of concentration is plotted against cumulative frequency (in percent) on an arithmetic probability scale. Elements whose concentrations in samples are lognormally distributed are considered to be present in anomalous amounts if sample concentrations exceed the arithmetic mean by two standard deviations ($\bar{x}+2\sigma$ criterion). The preceeding treatment of lognormally distributed data is not entirely appropriate. Transformation of lognormally distributed data to logarithms yields a normally distributed population for which mean, standard deviation, and $\bar{x}+2\sigma$ can be calculated. The antilogarithms of these values give estimates of the population's statistical tendencies. Calculating these parameters using untransformed data is significantly easier and provides a relatively accurate empirical estimate of a population's statistical tendencies. Further, if these parameters are

calculated for a weakly skewed lognormally distributed population such as that studied here, they will be similar to those calculated for the normal distribution curve that best fits the population.

The effect of calculating $\bar{x}+2\sigma$ in this fashion is to pick a threshold of lower concentration than would be calculated after transformation to logarithms. This mistake is preferable to picking too high a threshold concentration. As is subsequently demonstrated, the $\bar{x}+2\sigma$ criterion typically identifies too high a threshold, a situation that would be exacerbated by its rigorous calculation.

Certain characteristic departures from a lognormal distribution indicate that the threshold concentration for the studied distribution is a lower value (Lepeltier, 1969). If this is the case, one or more higher concentration populations may be superimposed on the background population, such as would be the case if samples from a mineralized area were included with a set of samples from an unmineralized area.

Superimposed populations may also result if the samples have been collected in very different geologic terranes, and therefore care must be taken to consider source terrane homogeneity for statistical treatment of data distributions. Although the threshold concentrations established here apply to the granitoid rocks of the eastern and southeastern Arabian Shield, they are probably grossly applicable in other areas underlain by calc-alkaline granitoid batholiths. Similar studies would be necessary to establish threshold values for the metamorphic terranes of the Arabian Shield.

Finally, some elements were present in such low concentrations or had such high minimum detection limits relative to average values that statistical treatment was impossible and any detected quantity is regarded as anomalous. This group of elements includes silver, gold, arsenic, bismuth, cadmium, antimony, zinc, and tungsten. No sample collected during this study contained detectable gold, antimony, arsenic, or cadmium.

Concentration versus cumulative frequency plots

Data for both rock and pan concentrate samples were compiled as the number of samples per concentration interval, then converted to cumulative frequency tables, one for each element, and evaluated. A cumulative frequency curve was plotted and visually evaluated for linearity. The mean plus two standard deviation rule was employed to establish threshold concentrations in linear cases (tables 3-5). In nonlinear cases an inflection point was picked and a computerized version of Sinclair's (1974) dual population resolution calculation was employed. In this method the positions of the

data points on the cumulative frequency distribution plot were recalculated in order to identify two distributions that, when combined, replicate the distribution of the total population. A plot of the two resolved frequency distribution curves (background and anomalous) was then produced. If the chosen inflection point did not yield a suitable population resolution, that is, if the resolution failed to produce two lognormally distributed populations, another inflection point was chosen and the procedure was repeated until a satisfactory result was obtained. Ideally, relatively straight lines were drawn through each set of recalculated points. The high-concentration background-population data point is identified as the threshold concentration; sample data that exceed this value are considered part of the anomalous population.

The principal assumption in this method is that the background source terrane is relatively homogeneous, that is, the geochemistry of the study area granitoids is relatively uniform. If this assumption is not valid, inflection points and threshold concentrations might be chosen that are artifacts of source terrane variation; such threshold concentrations would not correctly indicate the cutoff between mineralized and unmineralized rock. Threshold misidentification of this type typically results in a large percentage of samples being assigned to an anomalous population. Unless an unusually large number of samples were fortuitously collected within an anomalous area or the anomalous area is large relative to the entire area being sampled, the chosen inflection point will usually correspond to less than 10 percent and in some cases less than 5 percent of the total population.

Sinclair's (1974) method can also resolve total populations composed of three or more subpopulations, but the process is significantly more difficult. A simplified approach that is still relatively valid involves resolution of only the two highest concentration populations, that is, selection of the inflection point that gives the highest corresponding concentration. In most cases, the resolution so achieved is between the highest concentration background population and a suite of anomalous samples. Identification of these highest concentration populations (indicators of potentially mineralized rock) is the principal concern here. Small populations superposed at the low concentration end of the parent population may also be indicators of mineralized rock. The rock types being sought are usually identified by anomalously high concentrations of certain elements, but they may also be characterized by anomalously low, depleted concentrations of others.

INTERPRETATION OF GEOCHEMICAL DATA

Cumulative frequency distribution curves for pan concentrate and rock data are shown in figures 8 through 13. In these plots a break in slope and associated relative slope decrease indicate a greater number of samples in the intervals than predicted by the lognormal distribution. Conversely, a break in slope and relative slope increase represent fewer observations in the interval than predicted by the lognormal distribution.

Many of the plots have long tails at the low-concentration end of the population. These tails result from an unusually large number of samples in the interval immediately above the detection limit and probably represent reporting bias. Given the choice of reporting a numeric value or a numeric value qualified by less than (L) the analyst preferentially tends to choose the former. In pan concentrate samples, data for all elements except manganese, barium, chromium, vanadium, yttrium, and zirconium display this phenomenon. In rock samples, only manganese, barium, and zirconium data lack low-concentration tails. These tails were ignored during population resolution.

Pan concentrate samples

A brief discussion of the cumulative frequency plots follows. The results of population resolution for pan concentrates are graphically presented in figure 9, and threshold concentrations are listed in table 3.

Cumulative frequency data for manganese, boron, cobalt, molybdenum, scandium, strontium, and vanadium represent single lognormally distributed populations, and the Sinclair method was not applied. There may be a small manganese-depleted population superimposed on the low end of the total population, but the data set was too limited to model. The high concentration part of the boron population is sample depleted. The cobalt population includes one anomalously enriched sample (150 ppm), which caused a slight bend in an otherwise perfectly linear fit. Only 136 samples contained detectable molybdenum. This lognormal population is probably mostly anomalous and would be superimposed on the background population of 558 samples if the data distribution was more completely known.

The absence of strict linearity for vanadium data may also reflect on the precision of semiquantitative spectrographic data. Interpretation of cumulative frequency data for zirconium was hindered because half of all samples contained quantities of zirconium in excess of its maximum detection limit (1,000 ppm). No valid conclusions can be drawn except that the threshold concentration is greater than the maximum detection limit.

The data for strontium are a bit difficult to interpret, but several explanations are possible. First, cumulative frequency data for strontium may follow a distribution other than lognormal. Alternatively, strontium values may be lognormally distributed, but spectrographic analyses for strontium may have low precision relative to observed variance; this would render the characteristic distribution unidentifiable. Finally, the plot may be indicative of two superposed populations, each of which accounts for a substantial part of the full distribution, as is the case for the copper data. In this case, the concentration versus cumulative percent frequency distribution slopes would be nearly identical and there would be little data overlap between the two populations relative to concentration values. The latter would be evident on the frequency histograms but is not; therefore the strontium data probably do not represent two superposed populations.

Cumulative frequency data for barium, beryllium, chromium, copper, lanthanum, nickel, niobium, lead, tin, and yttrium are bimodal, and data for each bimodal distribution were resolved into two lognormally distributed subpopulations. Barium data show some fluctuations in the higher concentrations that render the resolution approximate. The interval reported as 1.5 ppm beryllium contained only 5 samples, whereas the adjacent intervals contained 137 and 176 samples. This appears to be another case of analytical bias, and the interval reported as 1.5 ppm was not employed. It appears that samples containing 1.5 ppm beryllium were not reported as such but rather as containing either 1 or 2 ppm beryllium. At the low-concentration end of the chromium distribution the departure from lognormality is not significant because the data points are the result of only two observations spread between the four lowest concentration intervals. The cumulative frequency distribution of copper is an interesting case. The population is resolved into two lognormal populations, and each accounts for half of the total population. It is not likely that half of the population is copper anomalous but rather that the pan concentrate data are from two very different copper populations. A reasonable petrologic explanation for this has not been determined. The data for niobium show a profound break above 500 ppm. There are only two classes containing data above this value so the Sinclair method cannot be applied. The break in the data is probably significant however, and a threshold concentration was identified on this basis.

In summary, the Sinclair method identified threshold concentration for beryllium, niobium, tin, and yttrium that are less than and statistically more rigorous than the threshold concentrations predicted by the $\bar{x}+2\sigma$ criterion.

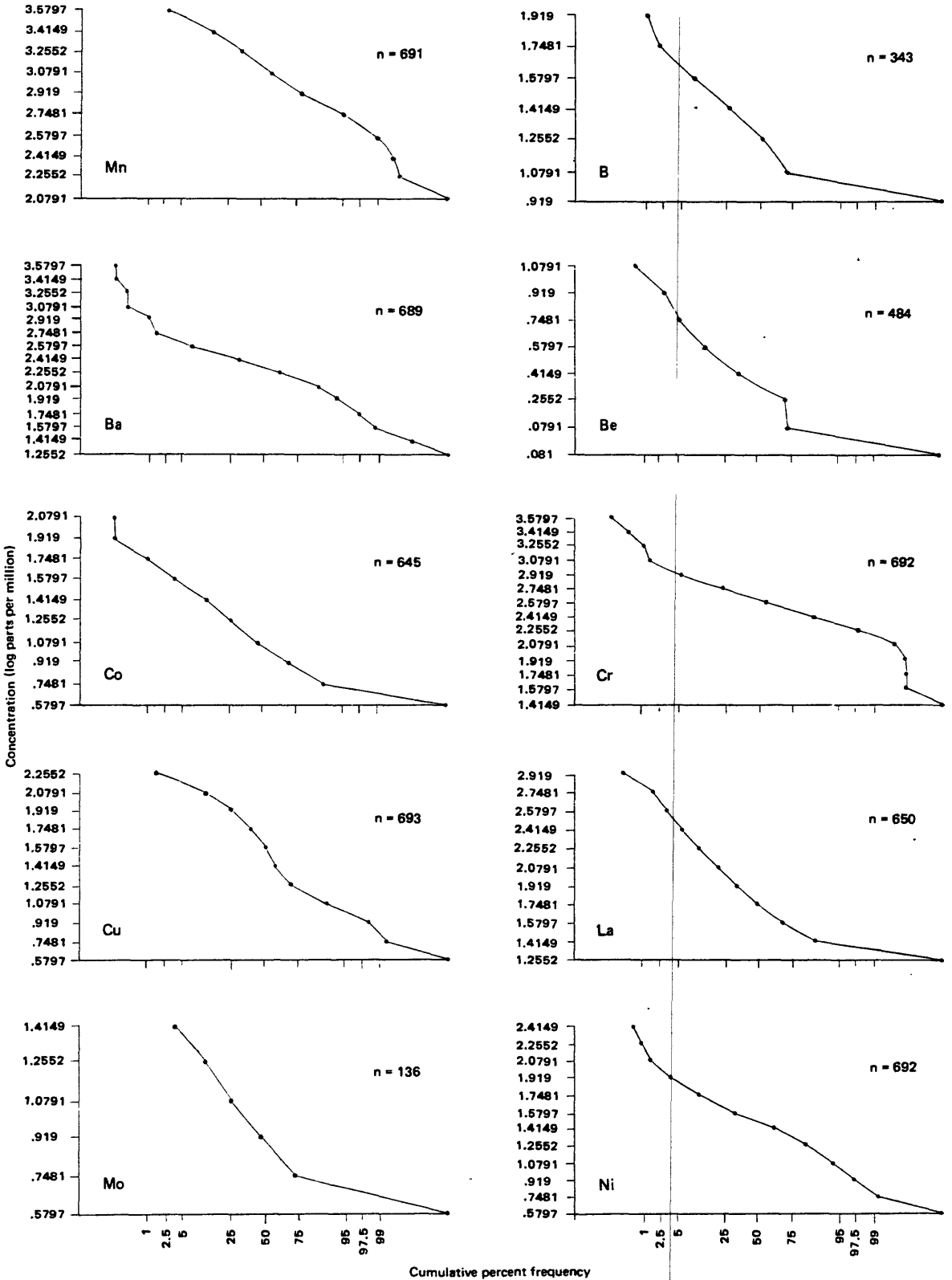

Figure 8.–Plots of the log of reporting intervals' lower concentration limits (semiquantitative spectrographic data, in parts per million) versus cumulative percent frequency (arithmetic probability scale), by element, for 694 pan concentrates collected in the eastern and southeastern Arabian Shield. n = the number of samples plotted, that is, those not qualified by either L (less than) or G (greater than).

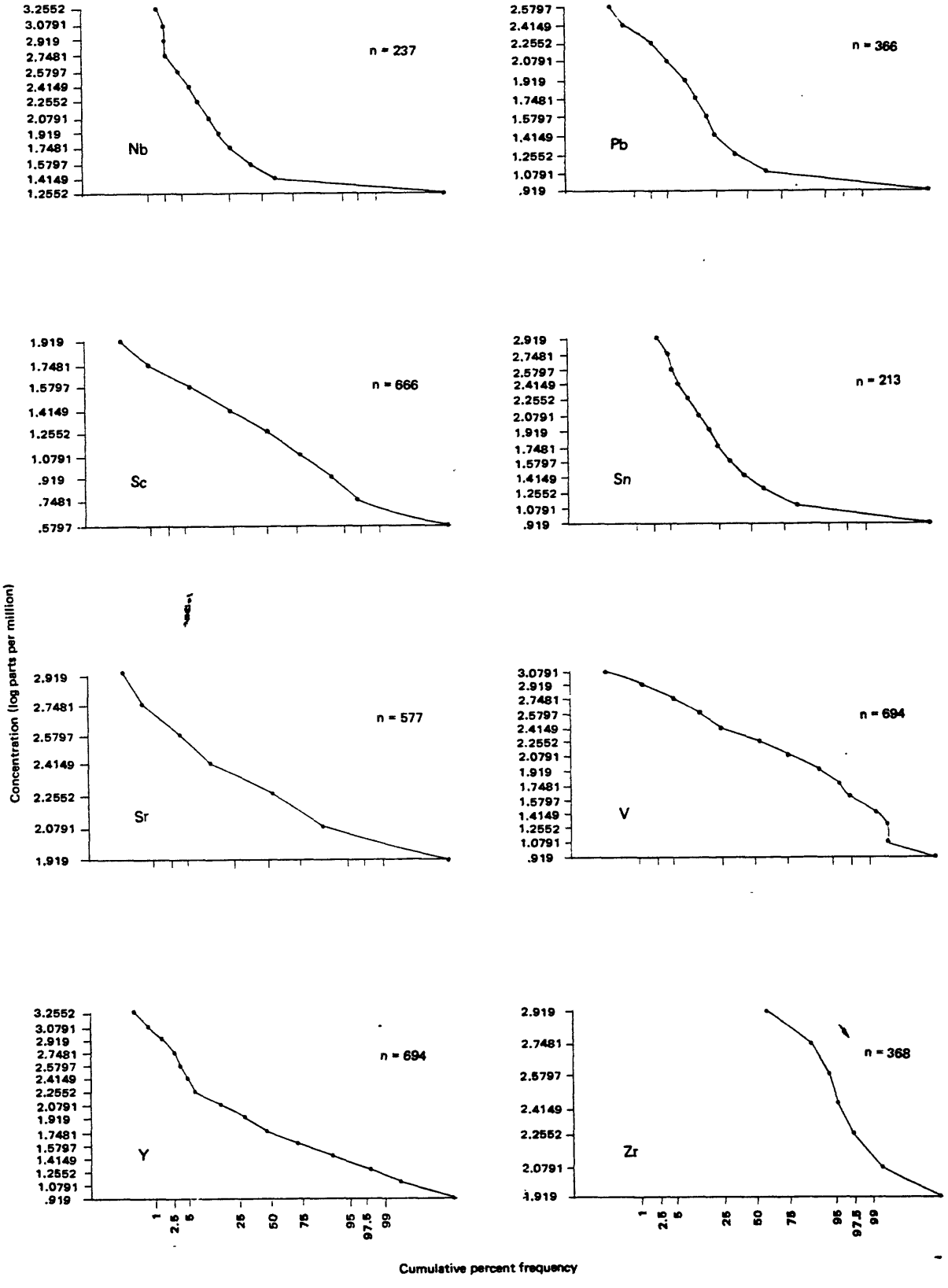

Figure 8.–Continued

Table 3.--*Statistical data and threshold concentrations of semiquantitative spectrographic data for pan concentrates*

[Only data not qualified by either L (less than) or G (greater than) were used in the calculations. Leaders indicate an element undetected in all samples. Values for Fe, Mg, Ca, and Ti in weight percent; all others in parts per million. N.C. indicates threshold concentration not calculated; see text]

Element	Detection limit	Number of values	Mean ($\bar{x}$)	Standard deviation (σ)	$\bar{x}+2\sigma$	Sinclair threshold concentration[2]	Threshold concentration[9]
Fe	0.05	672	8.8	4.8	18.4	3	N.C.
Mg	.02	694	1.5	1.2	4.7	3	N.C.
Ca	.05	694	3.0	1.6	6.6	3	N.C.
Ti	.002	261	0.8	0.2	1.2	3	N.C.
Mn	10	691	1,556	927	3,410	6	3,000
Ag	.5	0	—	—	—	4	0.5
As	200	0	—	—	—	4	200
Au	10	0	—	—	—	4	10
B	10	343	21	15	51	5	50
Ba	20	689	233	232	696	830	700
Be	1	484	3	2	7	4	5
Bi	10	26	27	20	1	5	15
Cd	20	0	—	—	—	4	20
Co	5	645	15	12	39	6	30
Cr	10	692	484	329	1,142	830	1,000
Cu	5	693	57	48	153	7	150
La	20	650	95	118	331	260	300
Mo	5	136	10	6	22	5	20
Nb	20	237	96	266	628	5008	500
Ni	5	692	36	31	98	83	100
Pb	10	366	33	48	129	83	100
Sb	100	0	—	—	—	4	100
Sc	5	666	20	11	42	6	50
Sn	10	213	94	202	498	180	200
Sr	100	577	190	88	366	6	300
V	10	694	233	181	595	6	500
W	50	14	96	51	198	4	50
Y	10	694	99	184	467	260	300
Zn	200	1	200	—	—	4	200
Zr	10	368	830	236	1,302	5	1,50010

1/ Insufficient unqualified data for valid application of $\bar{x}+2\sigma$ criterion; threshold concentration chosen by visual examination of frequency histogram.

2/ Sinclair (1974) threshold concentration is defined as the maximum concentration observed in the resolved background population.

3/ Deposits of these elements not expected nor are these elements indicators of the geochemical affinities being sought; Sinclair method not attempted.

4/ Any detected occurrence considered anomalous.

5/ Insufficient unqualified data for valid application of Sinclair method.

6/ Sinclair method indicates that the sample population is a single lognormally distributed population; the threshold concentration is defined as $\bar{x}+2\ \sigma$.

7/ Sinclair method resolves the copper population into two populations, each accounting for half of the parent population; see discussion in text.

8/ Sinclair plot portrays a distinct break between low and high concentration populations at 500 ppm; see text.

9/ The threshold concentration is defined as the lesser of either the spectrographic-reporting-interval midpoint corresponding to the interval's lower limit, identified by the Sinclair method, or the interval midpoint nearest the $\bar{x}+2\sigma$ criterion. Values greater than the threshold concentration are considered anomalous.

10/ The maximum detection limit for zirconium is 1,000 ppm. Because half of the samples exceed this value, no valid evaluation of zirconium concentrations in the pan concentrates can be made.

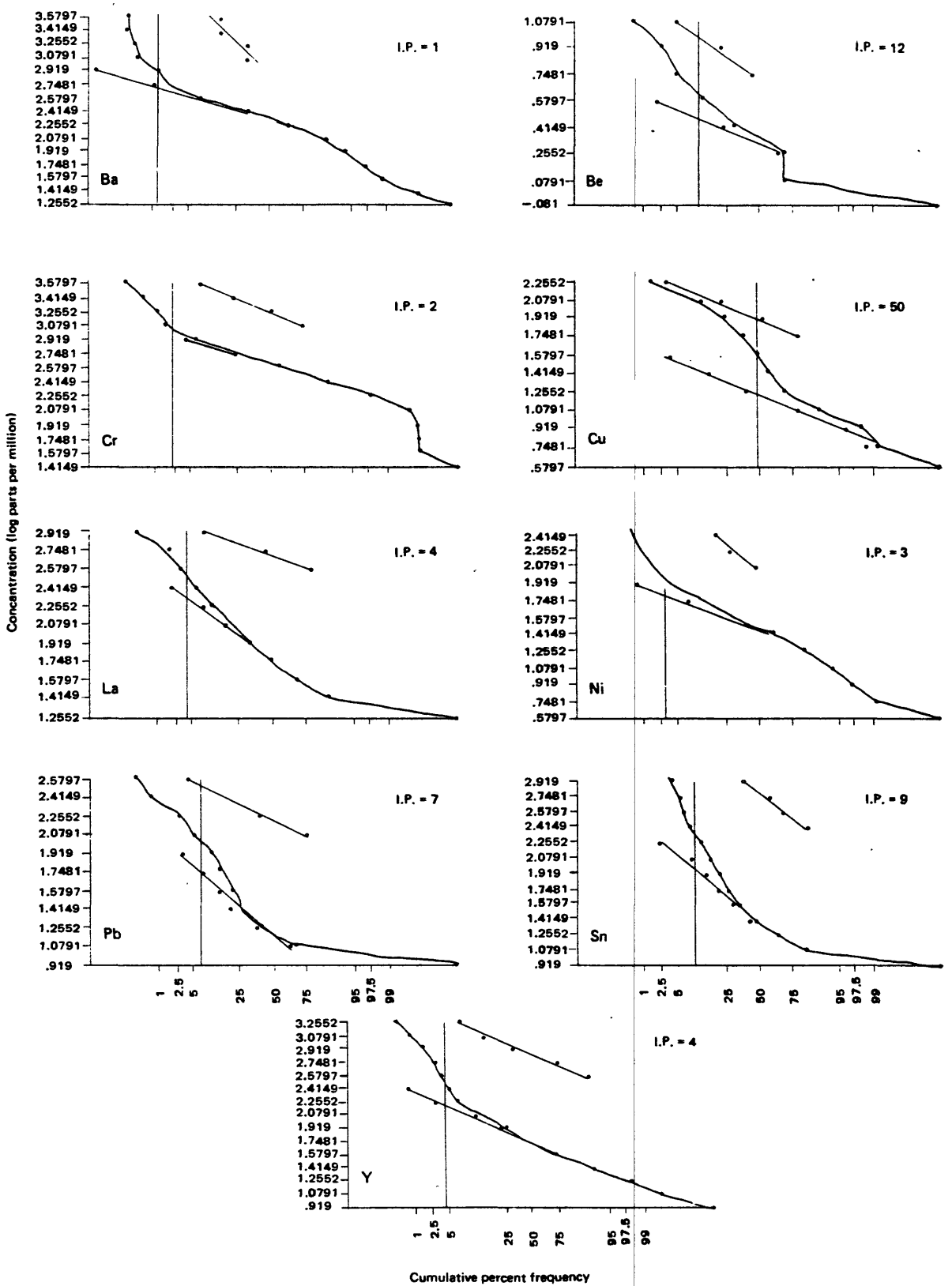

Figure 9.–Plots of log concentration semiquantitative spectrographic data versus cumulative percent frequency for pan concentrates. Only elements that show departures from lognormal distribution are displayed. The heavy curve represents all data in the sample population. The two light lines and the points represent the two lognormal populations resolved from the total population by the method of Sinclair (1974). The vertical line cutting the curves represents the inflection point (IP) picked for the resolution; I.P. indicates the percentage of the parent population formed by the higher concentration (anomalous) population. The lower concentration population is considered the background population.

Rock samples

Semiquantitative spectrographic data and quantitative data for lithium, fluorine, and tungsten

A brief discussion of the concentration versus cumulative frequency plots of semiquantitative and quantitative data for rock samples follows (fig. 10). The results of population resolution of these data are graphically presented in figure 11, and threshold concentrations are listed in table 4.

Cumulative frequency distributions for manganese, boron, lead, strontium, and zirconium in rock samples represent single lognormally distributed populations, and the Sinclair method was not applied. One sample contained 150 ppm boron and is significantly enriched relative to the remainder of the population. The lead data distribution is linear except for two samples, each of which contained 500 ppm lead. Strontium data also plot as a straight line. The zirconium frequency distribution has a lower correlation coefficient than the other lognormally distributed elements but is still interpreted to be linear.

Cumulative frequency data for barium, beryllium, cobalt, chromium, copper, lanthanum, molybdenum, nickel, niobium, scandium, tin, vanadium, yttrium, lithium, and fluorine are bimodal, and data for each bimodal distribution were resolved into two lognormally distributed subpopulations. The barium data may actually be trimodal, but resolution was attempted for the two higher concentration populations only. Beryllium data are not continuous at high concentration, and the resolution achieved is approximate. The copper data for rock samples are interesting, as they were for copper in pan concentrates. Again, the resolution achieved identified two copper populations, both of which are very large. The rock samples corroborate the observation that relative to copper content, two different granitoid clans are present in the eastern and southeastern Arabian Shield. No small anomalously enriched population (less than 10 percent of the full population) is resolvable from the higher concentration population. Only 100 of all rock samples analyzed contained detectable molybdenum, but this population was effectively resolved into background and anomalous populations. The threshold thus achieved seems to represent a valid cutoff between the background and anomalous populations (fig. 5). The nickel population was successfully resolved, but the distribution includes one highly anomalous sample that diverges from the anomalous population. Similarly, the niobium distribution was successfully resolved and includes a single, highly anomalous sample. Only 80 samples contained detectable tin. This population was resolved into two lognormal distributions, but the selected threshold concentration is probably too high as a result of the high detection limit (10 ppm) for

Table 4.--*Statistical data and threshold concentrations of semiquantitative spectrographic and quantitative data for rock samples*

[Only data not qualified by either L (less than) or G (greater than) were used in the calculations. Leaders indicate an element undetected in all samples. Values for Fe, Mg, Ca, and Ti in weight percent; all others in parts per million. N.C. indicates threshold concentration not calculated; see text]

Element	Detection limit	Number of values	Mean ($\bar{x}$)	Standard deviation (σ)	$\bar{x}+2\sigma$	Sinclair threshold concentration[2]	Threshold concentration[8]
Fe	0.05	695	2.0	1.8	5.6	[3]	N.C.
Mg	.02	641	0.65	1.2	3.1	[3]	N.C.
Ca	.05	696	1.6	1.7	5.0	[3]	N.C.
Ti	.002	668	.18	0.19	0.6	[3]	N.C.
Mn	10	693	431	333	1,097	[4]	N.C.
Ag	.5	52	2	4	10[1]	[5]	0.5
As	200	0	—	—	—	[5]	200
Au	10	0	—	—	—	[5]	10
B	10	175	15	12	39	[4]	30
Ba	20	606	555	492	1,539	829	1,000
Be	1	536	3	3.2	9	8	10
Bi	10	10	28	16	60[1]	[6]	10
Cd	20	0	—	—	—	[5]	20
Co	5	137	12	7	28	18	20
Cr	10	695	190	83	356	260	300
Cu	5	635	31	36	103	[7]	100
La	20	426	38	28	94	56	70
Mo	5	100	7	8	23	11	15
Nb	20	102	41	51	143	83	100
Ni	5	319	14	25	64	56	70
Pb	10	501	28	30	86	[4]	70
Sb	100	0	—	—	—	[5]	100
Sc	5	196	11	9	28	12	15
Sn	10	80	68	88	244[1]	[6]	15
Sr	100	390	312	233	776	[4]	700
V	10	605	40	49	138	56	70
W	50	2	175	—	[1]	[5]	50
Y	10	498	44	44	132	120	150
Zn	200	11	309	158	625[1]	[5]	200
Zr	10	685	151	162	473	[4]	500
Li		696	47	97	241	110	110
W		30	24	538	1,100[1]	[5]	10
F		696	837	962	2,760	1,900	1,900

Table 4 (Cont.)

1/ Insufficient unqualified data for valid application of $\bar{x}+2\sigma$ criterion; threshold concentration chosen by visual examination of frequency histogram.

2/ Sinclair (1974) threshold concentration is defined as the maximum concentration observed in the resolved background population.

3/ Deposits of these elements not expected nor are these elements indicators of the geochemical affinities being sought; Sinclair method not attempted.

4/ Sinclair method indicates that the sample population is a single lognormally distributed population, the threshold cxoncentration is therefore defined as $\bar{x}+2\sigma$.

5/ Any detected occurrence considered anomalous.

6/ Insufficient unqualified data for valid application of Sinclair method.

7/ Sinclair method resolves the copper population into two populations, each accounting for more than 30 percent of the parent population; see discussion in text.

8/ The threshold concentration is defined as the lesser of either the spectrographic-reporting-interval midpoint corresponding to the interval's lower limit, identified by the Sinclair method, or the interval midpoint nearest the $\bar{x}+2\sigma$ criterion. Values greater than the threshold concentration are considered anomalous.

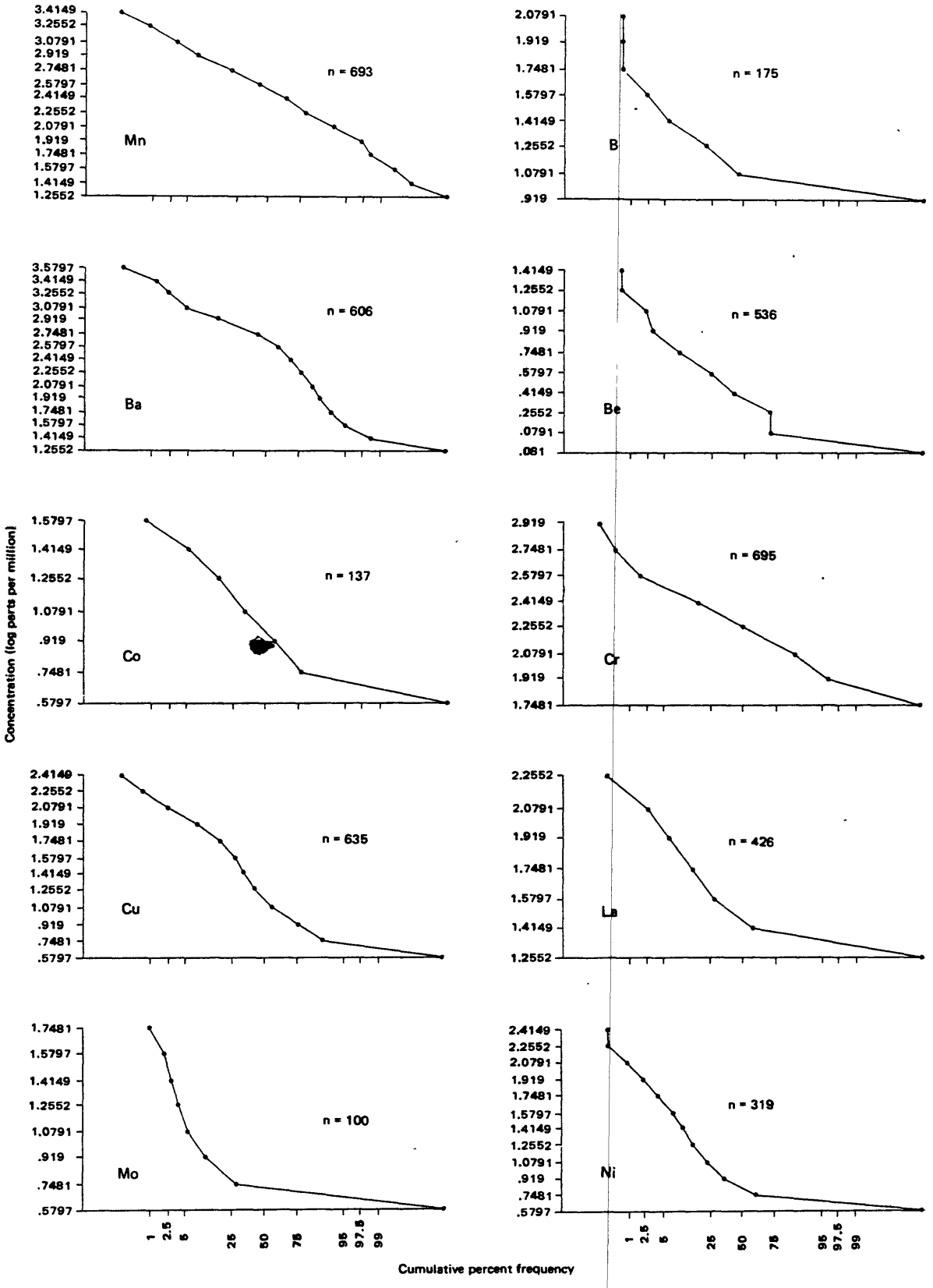

Figure 10.–Plots of the log of reporting intervals' lower concentration limits (semiquantitative spectrographic data, in parts per million) versus cumulative percent frequency (arithmetic probability scale), by element, for 696 rock samples collected in the eastern and southeastern Arabian Shield. Lithium and fluorine data were obtained by quantitative chemical analyses; the log of the lower limit of 10- and 100-ppm intervals, respectively, is plotted against cumulative percent frequency. n = the number of samples plotted, that is, those not qualified by either L (less than) or G (greater than).

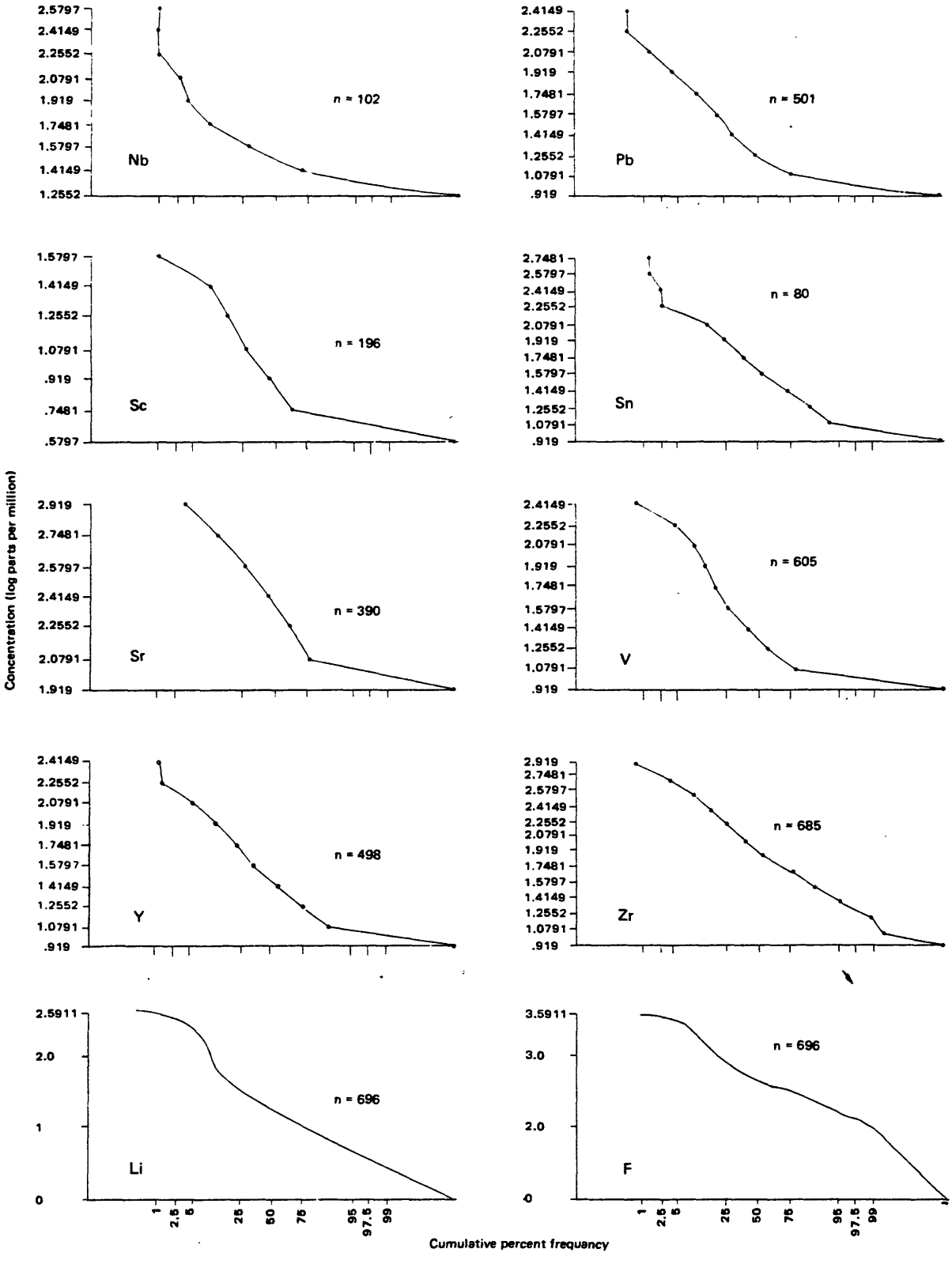

Figure 10.–Continued.

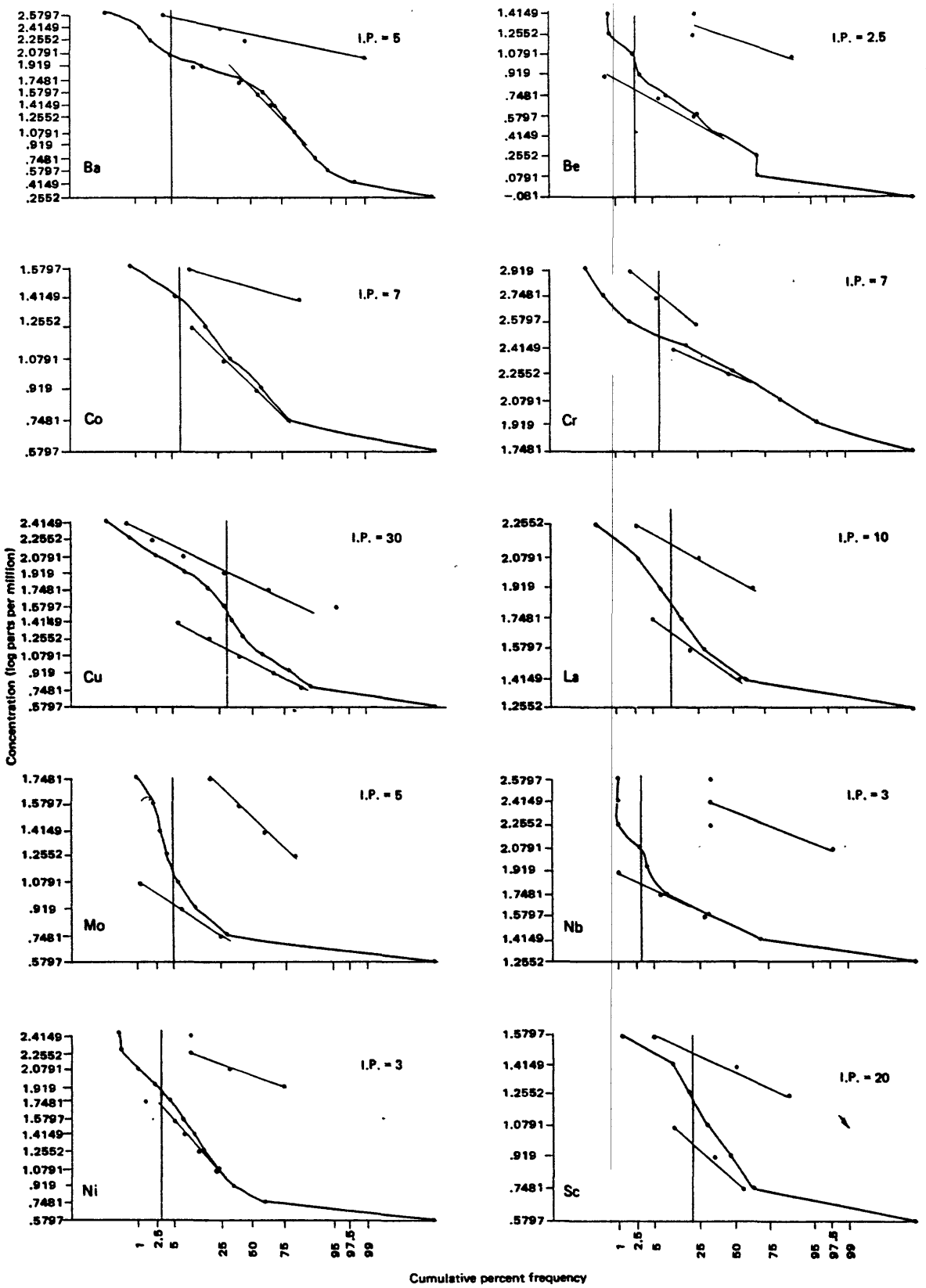

Figure 11.–Plots of log concentration semiquantitative spectrographic data versus cumulative percent frequency for rock samples. Only elements that show departures from log-normal distribution are displayed. The heavy curve represents all data in the sample population. The two light lines and the points represent the two lognormal populations resolved from the parent population by the method of Sinclair (1974). The vertical line cutting the curves represents the inflection point (I.P.) picked for the resolution; I.P. indicates the percentage of the parent population formed by the higher concentration (anomalous) population. The lower concentration population is considered the background population.

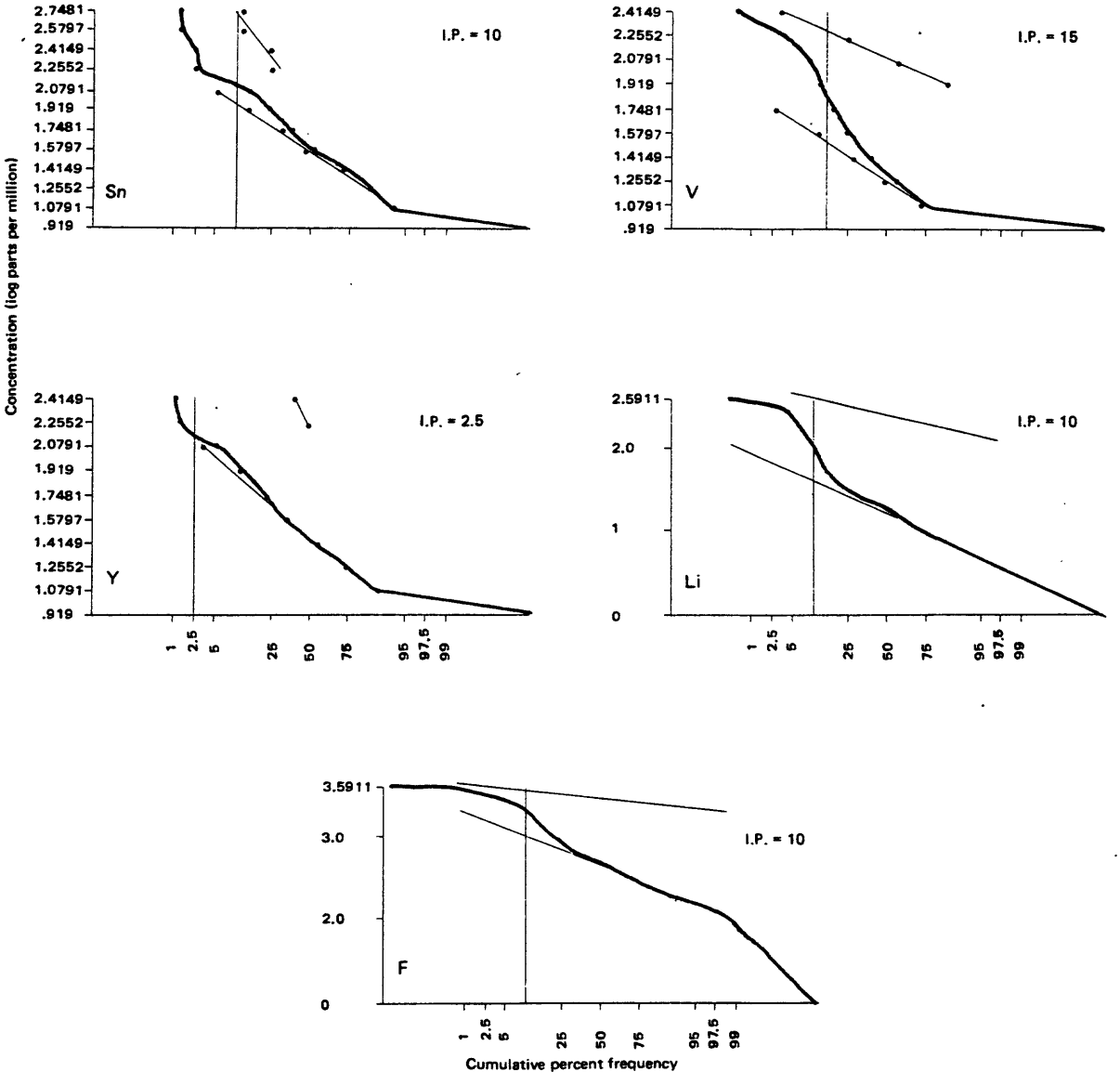

Figure 11.– Continued

tin (the worldwide average for tin in granitoids is about 3 ppm; Chappell and White, 1974). The resolution achieved here is most likely between superposed anomalous and very anomalous populations. The threshold concentration was chosen at 10 ppm, on the basis of the frequency histogram (fig. 10) and global averages. Resolution of the yttrium population yielded a very small anomalous population of six samples.

Quantitative data for lithium and fluorine were each effectively resolved into two lognormal populations. In the case of each element, 10 percent of the population belongs to a resolved anomalous population. Data points were not plotted on figures 10 and 11 because the data were reported continuously and sample points were sufficiently numerous at concentrations greater than 10 and 100 ppm, respectively, that they coalesced to a line.

Only 30 samples contained detectable tungsten as determined colorimetrically. This population is insufficiently large for statistical treatment, but all detected concentrations of tungsten are considered anomalous.

In summary, the Sinclair method identified threshold concentrations for barium, cobalt, lanthanum, molybdenum, niobium, scandium, vanadium, lithium, and fluorine that are less than the threshold concentrations predicted by the $\bar{x}+2\sigma$ criterion.

X-ray fluorescence data

Trace-element data for granitoid rocks are good indicators of their geochemical affinities, which in turn may provide information concerning the nature and likelihood of associated mineralized rocks. An X-ray fluorescence multichannel spectrometer was used to produce accurate, high-precision analyses for rubidium, strontium, yttrium, zirconium, and niobium. Using these elemental abundances, the plutons were separated into I- and S-type granites; this classification scheme helped predict the types of mineral deposits that are most likely to be found.

Frequency distribution data (fig. 5) were converted to cumulative frequency data and plotted against log of concentration (fig. 12). A brief discussion of the cumulative frequency plots of X-ray fluorescence data for rock samples follows. The results of population resolution are graphically presented in figure 13, and threshold concentrations are listed in table 5. Data points were not indicated on the plots because the data were reported continuously and sample points were sufficiently numerous that they coalesced to a line.

Table 5.--*Statistical data and threshold concentrations of X-ray fluorescence trace-element data for rock samples*
[Only data not qualified by either L (less than) or G (greater than are used in the calculations. All values in parts per million]

Element (detection limit)	Number of values	Mean ($\bar{x}$)	Standard deviation (σ)	$\bar{x}+2\sigma$	Sinclair threshold concentration[2]	Threshold concentration[4]
Rb (11)	627	158	172	502	350	350
Sr (10)	523	212	247	706[1] / -282	125	125
Y (9)	518	43	39	121	90	90
Zr (8)	681	144	141	426	[3]	426
Nb (6)	371	20	15	50	15	15
Rb/Sr	692	7.4	15	37.4	40	37

[1] The first figure represents $\bar{x}+2\sigma$ and the second figure represents $\bar{x}-2\sigma$; $\bar{x}-2\sigma$ predicts an anomalously depleted population.

[2] The Sinclair (1974) threshold concentration is defined as the maximum concentration observed in the background population or in the case of strontium, for which the anomalous population is strontium depleted, the minimum of the background population.

[3] Sinclair method indicates that the sample population is a single lognormally distributed population; the threshold concentration is therefore defined as $\bar{x}+2\sigma$

[4] The threshold concentration is defined as the lesser of the thresholds by $\bar{x}+2\sigma$ and the Sinclair methods, except for strontium, for which the threshold is the minimum value of the two threshold concentrations.

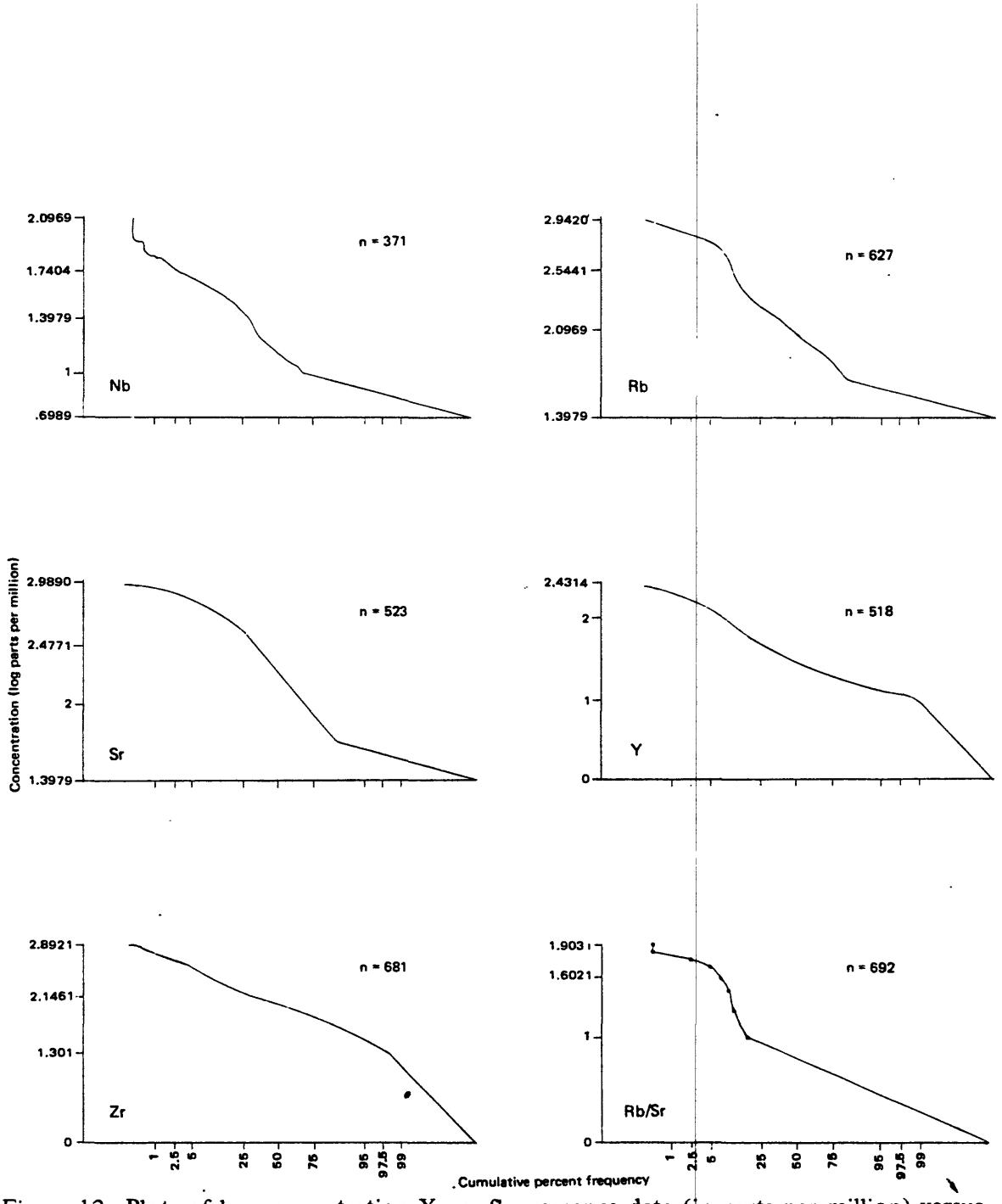

Figure 12.–Plots of log concentration X-ray fluorescence data (in parts per million) versus cumulative percent frequency (arithmetic probability scale), by element, for 692 rock samples collected in the eastern and southeastern Arabian Shield. Cumulative frequency is plotted against the log of the lower limit of 25-ppm intervals for rubidium and strontium, 10-ppm intervals for yttrium and Rb/Sr, 20-ppm intervals for zirconium, and 5-ppm intervals for niobium. n = the number of samples plotted, that is, those not qualified by either L (less than) or G (greater than).

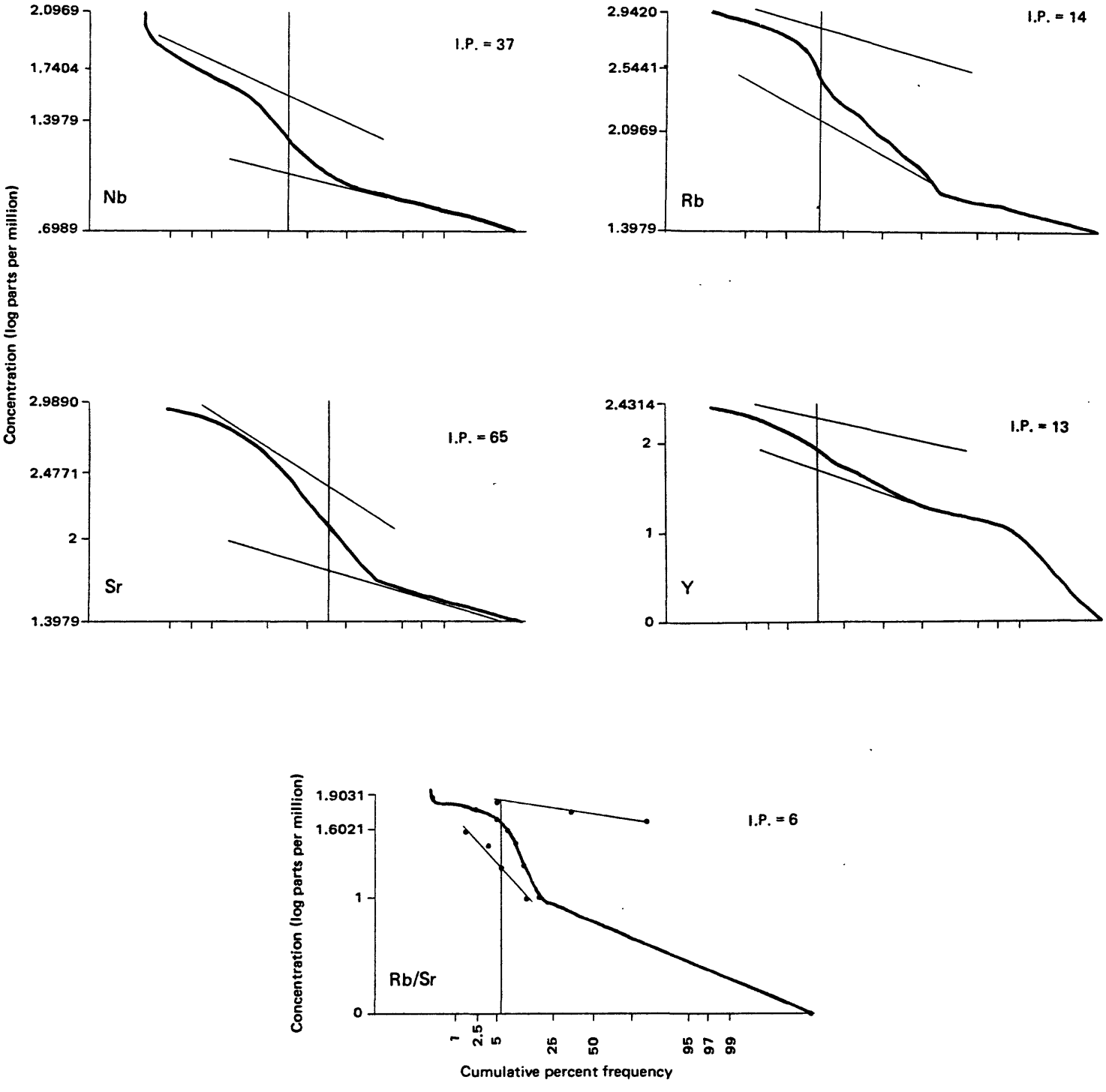

Figure 13.--Plots of log concentration X-ray fluorescence data versus cumulative percent frequency for rock samples. Only elements that show departures from lognormal distribution are displayed. The heavy curve represents all data in the sample population. The two light lines represent the two lognormal populations resolved from the total population by the method of Sinclair (1974). The vertical line cutting the curves represents the inflection point (I.P.) chosen for resolution; I.P. indicates the percentage of the total population formed by the higher concentration population. The lower concentration (anomalous) population is considered the background population, except for strontium, for which the lower concentration population is the anomalous one.

The cumulative frequency distribution of zirconium represents a single lognormally distributed population, and the correlation coefficient for the distribution is relatively high. The deviation portrayed at low concentrations is attributable to the approach of the detection limit. If a more accurate assessment of the distribution in the range from 0 to 20 ppm were possible, a more nearly linear plot would probably result.

Cumulative frequency data for niobium, rubidium, strontium, and yttrium and the Rb/Sr ratio are bimodal, and data for each bimodal distribution were resolved into two lognormally distributed populations. A quite satisfactory resolution of the niobium data was achieved. The anomalous population includes five extreme values.

The resolution achieved for the rubidium data is peculiar. The anomalous population is lognormally distributed and is characterized by a relatively high correlation coefficient. The background population, although approximated by a lognormal curve, may follow some other distribution. In this case, the threshold value is more accurately identified as the minimum value attributable to the anomalous population.

The strontium distribution is noteworthy because the anomalous population, that is, the smaller of the resolved populations, is a strontium-depleted population, as is typical for S-type granites. The low-concentration tail on the total strontium distribution indicates an unexpectedly large number of samples in this concentration range.

The cumulative frequency distribution for the yttrium data was effectively resolved. The deviation from linearity of the low-concentration population is attributable to the approach of the detection limit and a consequent loss of accuracy and precision. Fully 25 percent of the samples analyzed contained less than 5 ppm yttrium, and if a more accurate assessment of their distribution was achieved, a more linear plot in the low-concentration range would probably result.

The resolution achieved for the Rb/Sr ratio distribution is probably that between anomalous and highly anomalous populations. The threshold concentration of 40 is high relative to those found in global geochemical data compilations for granitoid rocks. (For example, Krauskopf (1967) indicates an Rb/Sr ratio of 0.53 for average granite). In fact, most granitoid rocks have a Rb/Sr ratio less than 1, as do more than 75 percent of the rock samples collected in the study area. Consequently, the resolution achieved in our study is of questionable value. A more meaningful threshold concentration for the Rb/Sr ratio probably is between 1 and 5.

The Sinclair (1974) method identified threshold concentrations for rubidium, strontium, yttrium, and niobium that are less than and statistically more rigorous than those identified by the $\bar{x}+2\sigma$ criterion. Because the zirconium distribution was unresolvable, the $\bar{x}+2\sigma$ criterion was used. For the Rb/Sr ratio, the $\bar{x}+2\sigma$ method actually predicted a lower threshold concentration (37) than the Sinclair method (40); therefore the former is used to evaluate the data.

GEOCHEMICAL ANOMALIES

All data values that exceed their respective threshold concentrations are plotted at their sampling locations (plates 1-3); these locations are considered to be anomalous in the indicated elements. At many locations samples were anomalous in only one or two elements (plates 1-3). Because samples from these locations do not include extreme values and are not part of regional anomalies, the anomalous character of these samples may be an artifact of panning, in the case of pan concentrates, or the result of localized geochemical variation.

Most areas that contain a group of samples anomalous in a single element are underlain by a granitoid that is geochemically atypical of the eastern and southeastern Arabian Shield but is probably not mineralized. For example, the granite and alkali granite of the Jabal al Hassir ring complex are enriched in lanthanum (plate 2) but not in any elements of economic significance. Many locations on plate 1 are characterized by samples anomalous in scandium, cobalt, vanadium, chromium, or manganese; these anomalies are probably attributable to greater than normal accumulations of oxide and ferromagnesian minerals in pan concentrates from those localities.

Anomalous areas are defined as those that contain samples that share an anomalous-element suite. The anomalous areas considered in this report are delineated on the basis of anomalous-element suites detected in one or more sample medium.

Geochemically anomalous areas are plotted and named on plates 1, 2, and 3. Some areas are anomalous on one plate but not on the others; some areas contain anomalous rock samples and nonanomalous pan concentrates, for example, the region underlain by the Jabal al Ehn monzogranite (plate 2). The most significant anomalous areas are those that appear on all three geochemical anomaly maps.

The plutonic source for each of these anomalous areas is geochemically distinct relative to the average eastern and southeastern Arabian Shield pluton, and together the sources form a geochemically discrete subset. Samples of the Jabal Sabhah monzogranite, Hassat ibyn Huwail granite, Jabal al

Hawshah monzogranite, Jabal as Sitarah monzogranite, Jabal Sahah granite, monzogranite near Jabal Tarban, monzogranite and granodiorite near Jabal Kebad, granite near Bir Masala, Jabal Bani Bwana granite, and Jabal al Gaharra monzogranite contain anomalous amounts of combinations of the elements lithium, fluorine, tin, beryllium, lead, yttrium, rubidium, and niobium, a suite typical of tin-mineralized granites (Tischendorf, 1977). Individual samples from certain of these plutons are enriched in tungsten, molybdenum, bismuth, zinc, or silver. Table 6 summarizes the geochemical differences between these plutons and the average granitoid rock in the study area and the similarities between these plutons and metallogenically specialized granitoids of the world.

Petrographic examinations were conducted to further characterize the plutons in these anomalous areas (table 2). The rocks are typically hypidiomorphic to xenomorphic, inequigranular, leucocratic monzogranites containing primary muscovite with or without biotite and garnet. These petrographic characteristics are the same as those described for S-type granites (Chappell and White, 1974). Both the petrography and trace-element chemistry of these plutons suggest that they are S-type granites, and the trace-element chemistry indicates that the small plutons that crop out at these localities have moderate favorability for deposits of tin, tungsten, or zinc.

Several other less significant anomalous regions were identified, including the isolated monzogranite jabals north of Jabal Sabhah, the Wadi Ghezm monzogranite south of Jabal al Gaharra, the granite and alkali granite in ring complexes at Jabal al Hassir and Jabal Ashira, the Najran alkali granite, the Jabal Bitran monzogranite, and the Wadi Tarib strontium-anomalous area. The first two regions display some of the geochemical characteristics common to metallogenically specialized granites but do not include anomalous concentrations of tin, tungsten, or molybdenum. As previously noted, the Jabal al Ehn monzogranite, the granodiorite near Jabal Mahail, the monzogranite near Wadi Tafshah, the granodiorite near Madhah, the monzogranite and granodiorite near Jabal Zayd, and the Wadi al Habbah granodiorite have petrographic features that suggest an affinity to the S-type granite clan, and yet they do not contain anomalous concentrations of tin, tungsten, or molybdenum. All of these plutons may represent precursors to tin mineralization, to use Tischendorf's (1977) nomenclature, and probably do not warrant further study.

Three rock samples from Jabal Bitran contained 20 ppm tungsten but do not display any other features that suggest that the pluton is metallogenically specialized. In fact, there are no pronounced tungsten anomalies in the study area. The only significant concentrations of tungsten (greater than 50 parts per million) are associated with the muscovite-

Table 6.--*Trace-element geochemistry of metallogenically specialized granites and nonspecialized granites*
[Number of samples on which averages are based follow unit designations in parentheses. Only data not qualified by N (not detected) or L (less than) were used in determining averages. Leaders indicate no data available]

	Semiquantitative spectrography								X-ray fluorescence				
	Ba	Be	Cu	La	Pb	Sn	Li*	F**	Rb	Sr	Y	Zr	Nb
Metallogenically specialized granite (Tischendorf, 1977)(962)	-	13+ 6	-	-	-	40+ 20	400+ 200	3,700+ 1,500	580+ 200	-	-	-	-
Granites thought to be precursors to tin mineralization (Tischendorf, 1977) (226)	-	7.5+ 2	-	-	-	10+ 5	130+ 50	810+ 200	250+ 50	-	-	-	-
Granites (Krauskopf, 1967)(2,327)	600	5	10	40	20	3	30	850	150	285	40	180	20
Average for all samples from study area (696)	555	3	31	39	28	<10	47	836	158	212	43	144	20
Jabal Sabhah monzogranite (18)	<20	5.7	15	<20	54	<10	85	2,016	254	17	120	97	23
Hassat ibyn Huwail granite (16)	51	4	10	<20	20	<10	38	1,513	192	32	89	131	25
Jabal al Hawshah monzogranite (13)	109	4	34	<20	24	11	114	1,943	388	53	70	98	18
Jabal as Sitarah monzogranite (36)	26	6	14	<20	76	38	149	2,512	436	11	62	62	31
Jabal Sahah granite (15)	106	8	6	24	48	<10	61	2,083	227	22	109	136	46
Granite near Bir Masala (23)	111	4	22	21	40	<10	42	2,221	212	45	67	123	50
Monzogranite near Jabal Tarban (35)	188	7	12	51	55	24	67	1,176	369	33	53	76	25
Monzogranite and granodiorite near Jabal Kebad (5)	26	7	12	<20	22	23	52	1,117	292	12	<9	22	15
Jabal Bani Bwana granite (16)	<20	7	<5	<20	84	38	215	1,356	403	11	59	71	27
Jabal al Gaharra monzogranite (48)	<20	5	13	<20	30	75	300	3,126	573	<10	71	60	34

* Lithium determined by atomic absorption.
** Fluorine determined by the selective-ion-electrode method.

bearing leucomonzogranites mentioned above. These plutons all require further study with regard to the possibility of their containing tungsten deposits. Few other samples contained tungsten; their distribution is scattered, and they contained such small quantities of tungsten that additional investigations should be deferred.

Three of the alkali granites exposed in the study region, those at Jabal al Hassir, Jabal Ashirah, and west of Najran, contained anomalous amounts of the trace elements lanthanum, zirconium, fluorine, and niobium and were noticeably depleted in strontium. These observations correlate well with other studies of Arabian Shield alkali granites (Drysdall, 1979; Douch and Drysdall, 1980) and with experimental studies on enrichment of zirconium and rare earth elements in peralkaline melts (Watson, 1979). However, neither the radiometric nor geochemical results for these plutons suggest that they contain mineral deposits. Some additional fieldwork may be warranted to insure that no rare earth element-enriched microgranitic apophyses, such as those found in the northwest Hijaz (Drysdall, 1979; Douch and Drysdall, 1980), are associated with these larger peralkaline bodies.

RADIOMETRIC ANOMALIES

Radioactivity data (fig. 2) indicated only three areas in which the radiation detected was significantly above the background level. The total-count rates for the Jabal Sabhah monzogranite and the granite near Bir Masala were twice the average value observed for granitoid rocks of the study area. The count rate at Jabal al Hawshah is intermediate between the average value and those found at the two locations just mentioned. Otherwise, no significant radiometric anomalies were identified in the felsic plutonic rocks of the eastern and southeastern Arabian Shield.

CONCLUSIONS AND RECOMMENDATIONS

Most of the several hundred plutons that crop out in the eastern and southeastern Arabian Shield are not metallogenically specialized, and it is improbable that undiscovered ore deposits are associated with them. Of the 21 plutons considered to have mineral-deposit potential based on their petrographic characteristics (fig. 1, table 2), only 10 of them have associated geochemical anomalies: the Jabal Sabhah monzogranite, the Hassat ibyn Huwail granite, the Jabal al Hawshah monzogranite, the Jabal as Sitarah monzogranite, the Jabal Sahah granite, the monzogranite near Jabal Tarban, the monzogranite and granodiorite near Jabal Kebad, the granite near Bir Masala, the Jabal Bani Bwana granite, and the Jabal al Gaharra monzogranite. This group of postorogenic S-type granites has considerable potential for deposits of tin, tungsten, molybdenum, or zinc. Isolated or single-element geochemical anomalies are probably not significant.

The S-type granites of the study area should be intensively sampled and geologically mapped at large scale. Fieldwork should concentrate on identification of greisenized stockwork and quartz-vein systems such as that identified at Baid al Jimalah (Cole and others, 1981). The stockwork at Baid al Jimalah is associated with a small peraluminous S-type granite similar in many respects to several of those identified in the eastern and southeastern Arabian Shield, except that at Baid al Jimalah significant quantities of wolframite and cassiterite are exposed.

In their studies of deposits associated with S-type granites, Groves and McCarthy (1978) suggested that although lode deposits of tin and tungsten typically are located in the apical regions of mineralized stocks, deposits may also be localized well within a crystallizing magma in fractures that form during cooling. The trace-element geochemistry of the S-type granites discussed here suggests that they have potential for deposits of tin although no deposits have been identified. Perhaps, as Groves and McCarthy (1978) suggested, mineralized rocks in the form of lode deposits are located beneath the currently exposed level. Test drilling of the most promising of these plutons is advisable.

The radiometric anomalies identified may require follow-up work as well. Ground radiometric traverses should be completed coincident with geologic mapping. A thorough search for pegmatites and microgranitic apophyses should be conducted as these are possible loci for deposits of uranium, thorium, and rare earth elements.

REFERENCES

Ahrens, L. H., 1957, The log-normal distribution of the elements--a fundamental law of geochemistry and its subsidiary [Pt. 3]: Geochimica et Cosmochimica Acta, v. 11, no. 4, p. 205-212.

Chappell, B. W., and White, A. J. R., 1974, Two contrasting granite types: Pacific Geology, v. 8, p. 173-174.

Cole, J. C., Smith, C. W., and Fenton, M. D., 1981, Preliminary investigation of the Baid al Jimalah tungsten deposit, Kingdom of Saudi Arabia: U.S. Geological Survey Saudi Arabian Mission Technical Record 20 (Interagency Report 377), 26 p.; also, 1981, U.S. Geological Survey Open-File Report 81-1223.

Dodge, F. C. W., 1973, Geology and evaluation of tungsten anomalies Buhairan-Abu Khurg area, sotheastern part of the Uyaijah ring structure, Kingdom of Saudi Arabia: U.S. Geological Survey Saudi Arabian Project Report 163, 32 p.; also, 1973, U.S. Geological Survey Open-File Report (IR)SA-163.

Dodge, F. C. W., and Helaby, A. M., 1975, Mineralization in the Uyaijah-Thaaban area, west-central part of the Uyaijah ring structure, Kingdom of Saudi Arabia: U.S. Geological Survey Saudi Arabian Project Report 191, 43 p.; also, 1975, U.S. Geological Survey Open-File Report 75-175.

Douch, C. J., and Drysdall, A. R., 1980, The geology and resource potential of the Jabal Tawlah radioactive microgranite, NW Hijaz: Saudi Arabian Directorate General of Mineral Resources Open-File Report 694,34 p.

Drysdall, A. R., 1980, Petrogenesis of two peralkaline microgranites from NW Hijaz; some considerations relevant to further prospecting: Saudi Arabian Directorate General of Mineral Resources Open-File Report 705, 47 p.

du Bray, E. A., 1981, Evaluation of geochemical sampling media in granitoid terrane of the southern Arabian Shield, Kingdom of Saudi Arabia: U.S. Geological Survey Saudi Arabian Mission Miscellaneous Document 37 (Interagency Report 379), 8 p.; also, 1981, U.S. Geological Survey Open-File Report 81-1293.

_____ 1982, Peraluminous granites of the eastern Arabian shield, Kingdom of Saudi Arabia [abs.]: Precambrian Research, v. 16, no. 4, p. A16.

Elliott, J. E., *in press*, Tin-bearing granite of Jabal al Gaharra in the southern Arabian Shield, Kingdom of Saudi Arabia: Saudi Arabia Directorate General of Mineral Resources Bulletin

Fleck, R. J., Greenwood, W. R., Hadley, D. G., Anderson, R. E., and Schmidt, D. L., 1980, Age and evolution of the southern part of the Arabian Shield, in Evolution and mineralization of the Arabian-Nubian Shield: King Abdulaziz University, Institute of Applied Geology Bulletin 3, v. 3: Pergamon Press, Oxford-New York, p. 1-18.

Greenwood, W. R., and Brown, G. F., 1973, Petrology and chemical analysis of selected plutonic rocks from the Arabian Shield Kingdom of Saudi Arabia: Saudi Arabian Directorate General of Mineral Resources Bulletin 9, 9 p.

Greenwood, W. R., Anderson, R. E., Fleck, R. J., and Roberts, R. J., 1980, Precambrian geologic history and plate tectonic evolution of the Arabian Shield: Saudi Arabian Directorate General of Mineral Resources Bulletin 24, 35 p.

Greenwood, W. R., Stoeser, D. B., Fleck, R. J., and Stacey, J. S., 1982 Late Proterozoic island-arc complexes and tectonic belts in the southern part of the Arabian Shield, Kingdom of Saudi Arabia: Saudi Arabian Deputy Ministry for Mineral Resources Open-File Report USGS-OF-02-8, 46 p. ; also, 1983, U.S. Geological Survey Open-File Report 83-296, (IR)SA-433.

Groves, D. I., and McCarthy, T. S., 1978, Fractional crystallization and the origin of tin deposits in granitoids: Mineralium Deposita, v. 13, p. 11-26.

Hawkes, H. E., and Webb, J. S., 1962, Geochemistry in mineral exploration: New York, Harper and Row, 415 p.

Krauskopf, K. B., 1967, Introduction to geochemistry: New York, McGraw-Hill, 721 p.

Lepeltier, Claude, 1969, A simplified statistical treatment of geochemical data by graphical representation: Economic Geology, v. 64, no. 5, p. 538-550.

Miesch, A. T., 1967, Methods of computation for estimating geochemical abundance: U.S. Geological Survey Professional Paper 574-B, p. 1-15.

Overstreet, W. C., 1978, A geological and geochemical reconnaissance of the Tathlith one-degree quadrangle, sheet 19/43, Kingdom of Saudi Arabia: U.S. Geological Survey Saudi Arabian Project Report 230, 132 p.; also, 1978, U.S. Geological Survey Open-File Report 78-1072.

Schmidt, D. L., Hadley, D. G., and Stoeser, D. B., 1979, Late Proterozoic crustal history of the Arabian Shield, southern Najd province, Kingdom of Saudi Arabia, in Evolution and mineralization of the Arabian-Nubian Shield: King Abdulaziz University Institute of Applied Geology Bulletin 3, v. 2; Pergamon Press, Oxford-New York, p. 41-58.

Sinclair, A. J., 1974, Selection of threshold values in geochemical data using probability graphs: Journal of Geochemical Exploration, v. 3, p. 129-149.

Stoeser, D. B., and Elliott, J. E., 1980, Post-orogenic peralkaline and calc-alkaline granites and associated mineralization of the Arabian Shield, Kingdom of Saudi Arabia, in Evolution and mineralization of the Arabian-Nubian Shield: King Abdulaziz University, Institute of Applied Geology Bulletin 3, v. 4: Pergamon Press, Oxford-New York, p. 1-23.

Streckeisen, Albert, 1976, To each plutonic rock its proper name: Earth-Science Reviews, v. 12, p. 1-33.

Theobald, P. K., Jr., 1970, Al Kushamiya as a target for a Colorado-type molybdenite deposit, Southern Najd quadrangle, Kingdom of Saudi Arabia: U.S. Geological Survey Saudi Arabian Project Report 120, 13 p.; also, 1971, U.S. Geological Survey Open-File Report (IR)SA-120.

Theobald, P. K., and Allcott, G. H., 1973, Tungsten anomalies in the Uyaijah ring structure, Kushaymiyah igneous complex, Kingdom of Saudi Arabia, with a section on Regional geophysics, by V. J. Flanigan and G. E. Andreasen: U.S. Geological Survey Saudi Arabian Project Report 160, 86 p.; also, 1975, U.S. Geological Survey Open-File Report 75-657.

Tischendorf, G., 1977, Geochemical and petrographic characteristics of silicic magmatic rocks associated with rare-element mineralization, in Stemprok, M., and others, eds., Metallization associated with acid magmatism: Czechoslovakia Geological Survey, Prague, v. 2, p. 41-96.

U.S. Geological Survey (Saudi Arabian Mission), 1980, Index map of published 1:100,000-scale geologic maps: U.S. Geological Survey Saudi Arabian Mission Miscellaneous Map 100 (Interagency Report 400), scale 1:2,000,000; also, 1982, U.S. Geological Survey Open-File Report 82-289.

U.S. Geological Survey and Arabian American Oil Company, 1963, Geologic map of the Arabian Peninsula: U.S. Geological Survey Miscellaneous Geologic Investigations Map I-270 A, scale 1:2,000,000.

Watson, E. B., 1979, Zircon saturation in felsic liquids: experimental results and applications to trace element geochemistry: Contributions to Mineralogy and Petrology, v. 70, p. 407-419.

Whitlow, J. W., 1968a, Geology and geochemical reconnaissance of the Jabal Sahah quadangle, Southern Najd: Saudi Arabian Directorate General of Mineral Resources Mineral Investigations Map MI-14, scale 1:100,000.

_____ 1968b, Geology and geochemical reconnaissance of the Jabal ash Shumrah quadrangle, Southern Najd: Saudi Arabian Directorate General of Mineral Resources Mineral Investigations Map MI-15, scale 1:100,000.

_____ 1968c, Geology and geochemical reconnaissance of the Jabal al Hawshah quadrangle, Southern Najd: Saudi Arabian Directorate General of Mineral Resources Mineral Investigations Map MI-16, scale 1:100,000.

_____ 1968d, Geology and geochemical reconnaissance of the Al Kushaymiya quadrangle, Southern Najd: Saudi Arabian Directorate General of Mineral Resources Mineral Investigations Map MI-17, scale 1:100,000.